

THESIS

1

2004

3240

**LIBRARY
Michigan State
University**

This is to certify that the
thesis entitled

TOWARDS THE DEVELOPMENT OF SPATIALLY
UNBIASED LANDSCAPE FRAGMENTATION INDICES

presented by

Dante Gideon K. Vergara

has been accepted towards fulfillment
of the requirements for the

M.A. degree in Geography



Major Professor's Signature

Oct 16 2003

Date

PLACE IN RETURN BOX to remove this checkout from your record.
TO AVOID FINES return on or before date due.
MAY BE RECALLED with earlier due date if requested.

DATE DUE	DATE DUE	DATE DUE

TOWARDS THE DEVELOPMENT OF SPATIALLY UNBIASED LANDSCAPE
FRAGMENTATION INDICES

By

Dante Gideon K. Vergara

A THESIS

Submitted to
Michigan State University
in partial fulfillment of the requirements
for the degree of

MASTER OF ARTS

Department of Geography

2003

ABSTRACT

TOWARDS THE DEVELOPMENT OF SPATIALLY UNBIASED LANDSCAPE FRAGMENTATION INDICES

By

Dante Gideon K. Vergara

Most current landscape indices suffer from the effects of scale, precluding comparative studies between sites and/or with other continuous data over the landscape. A new index to describe landscape fragmentation as a spatial process based on patch density, patch shape complexity, and patch arrangement is proposed. The maximum support size encompassing a single spatial process centered on a point is determined by detecting changes in spatial structure as nested supports increases, through changes in significance of Moran's I and Geary's C as well as a changes in the structure of the variogram model. The support size over which to compute the fragmentation index now has basis and need not be arbitrary. The vertices of the polygon and its minimum spanning tree define the locations where the fragmentation index should be computed. Spatial interpolation on the indices derived at these selected points would generate the landscape fragmentation intensity surface, converting the initially discrete index into a continuous variable. Doing so will allow for comparative studies between sites and/or with other continuous data. Relating patterns to processes on the landscape would then be feasible. The methodology was tested on co-incident, classified ETM+ and Ikonos imagery of the Legal Amazon forest near Uruara, Para in Brazil.

Dedicated to my family

ACKNOWLEDGEMENTS

To my mentors:

Percy, Michael, and Ben,

For starting me on this line of scholarship;

Bob, Ashton, and Qi,

For their instruction, encouragement, comments, and kind words;

And in memory of my Dad,

Who taught me to think of possibilities;

THANK YOU ALL.

TABLE OF CONTENTS

LIST OF TABLES	viii
LIST OF FIGURES	ix
INTRODUCTION	1
I. Patterns and processes	3
II. Landscape fragmentation indices	4
III. Scale	6
IV. The bias of scale	7
V. Limitations of the current landscape fragmentation indices	9
VI. Statement of problem	10
VII. Objectives	11
VIII. Fragmentation	11
A. Patch density, arrangement and shape complexity	12
B. Estimates of index parameters	14
C. Development of the proposed index	17
IX. Overcoming the bias of spatial support	19
A. Smoothing the surface	19
1. Low pass or mean filter	19
2. Pycnophylatic interpolations	20
3. Kriging	21
B. Spatial processes	22

1. Areal approach	22
2. Point estimation approach	23
C. Generating the fragmentation intensity surface	24
MATERIALS AND METHODS	25
I. Satellite imagery	25
II. Nested supports	28
III. Fragmentation index	28
IV. Variograms and first lag gammas	29
V. Autocorrelation	31
VI. Regressions	31
RESULTS AND DISCUSSIONS	33
I. Fragmentation index	33
II. Moran's I and Geary's C	34
III. Variogram modelling	35
IV. Encompassing spatial processes	37
V. Estimating for null support	38
CONCLUSIONS	41
I. Areal approach	42
II. Point estimation approach	45
RECOMMENDATIONS	49
APPENDICES	52
APPENDIX A: Summaries for Fragmentation Parameters and Indices	53
APPENDIX B: Summaries for Increasing Support of Fragmentation Study	56

APPENDIX C: Variograms for Increasing Supports of Two Cases Each of Three Forest Scenarios	62
LITERATURE CITED	81
REFERENCES	85

LIST OF TABLES

Table 1. Non-redundant univariate landscape fragmentation indices (Riitters et al 1995).	5
Table 2. Summarized slope and intercept estimates with standard errors.	40
Table A.1.a. Forested 1	53
Table A.1.b. Forested 2	53
Table A.2.a. Non-Forested 1	54
Table A.2.b. Non-Forested 2	54
Table A.3.a. Intermediate 1	55
Table A.3.b. Intermediate 2	55

LIST OF FIGURES

Figure 1.1. Increasing number and sizes of patches	13
Figure 1.2. Uniform, random, and clustered patches	13
Figure 1.3. Patch shape complexity	14
Figure 2. Pycnophylactic interpolation	21
Figure 3. Satellite imagery, Uruara in the Legal Amazon, showing forest fragmentation at different resolutions.	26
Figure 4. Typical increasing support for fragmentation study	27
Figure 5. Typical variogram with exponential model showing nugget, sill and range variances.	30
Figure 6.1. Non-forested 1, 17 x 17 pixels	33
Figure 6.2. Non-forested 2, 17 x 17 pixels	33
Figure 7.1 First lag gamma and support size for six supports.	36
Figure 7.2 Ratio of first lag gamma and variance vs support size for six supports.	37
Figure 8. Typical areal estimation.	44
Figure 9.1. Non-convex hull polygons with centroids and vertices.	46
Figure 9.2. Internal vertices determined for spanning tree	46
Figure 9.3. Typical spanning tree within the polygon.	46
Figure 9.4. Thiessen triangles for surface generation	46
Figure 10. Typical point estimation	48
Figure B.1.a. Summaries of increasing support for fragmentation study: forested 1	56
Figure B.1.b. Summaries of increasing support for fragmentation study: forested 2	57

Figure B.2.a. Summaries of increasing support for fragmentation study: non-forested 1	58
Figure B.2.b. Summaries of increasing support for fragmentation study: non-forested 2	59
Figure B.3.a. Summaries of increasing support for fragmentation study: intermediate 1	60
Figure B.3.b. Summaries of increasing support for fragmentation study: intermediate 2	61
Figure C.1.1.a. Forested 1, 17 x 17 cells	63
Figure C.1.1.b. Forested 1, 33 x 33 cells	63
Figure C.1.1.c. Forested 1, 50 x 50 cells	64
Figure C.1.1.d. Forested 1, 67 x 67 cells	64
Figure C.1.1.e. Forested 1, 83 x 83 cells	65
Figure C.1.1.f. Forested 1, 100 x 100 cells	65
Figure C.1.2.a. Forested 2, 17 x 17 cells	66
Figure C.1.2.b. Forested 2, 33 x 33 cells	66
Figure C.1.2.c. Forested 3, 50 x 50 cells	67
Figure C.1.2.d. Forested 2, 63 x 63 cells	67
Figure C.1.2.e. Forested 2, 83 x 83 cells	68
Figure C.1.2.f. Forested 2, 100 x 100 cells	68
Figure C.2.1.a. Non-forested 1, 17 x 17 cells	69
Figure C.2.1.b. Non-forested 1, 33 x 33 cells	69
Figure C.2.1.c. Non-forested 1, 50 x 50 cells	70
Figure C.2.1.d. Non-forested 1, 67 x 67 cells	70
Figure C.2.1.e. Non-forested 2, 83 x 83 cells	71

Figure C.2.1.f. Non-forested 1, 100 x 100 cells	71
Figure C.2.2.a. Non-forested 2, 17 x 17 cells	72
Figure C.2.2.b. Non-forested 2, 33 x 33 cells	72
Figure C.2.2.c. Non-forested 2, 50 x 50 cells	73
Figure C.2.2.d. Non-forested 2, 67 x 67 cells	73
Figure C.2.2.e. Non-forested 2, 83 x 83 cells	74
Figure C.2.2.f. Non-forested 2, 100 x 100 cells	74
Figure C.3.1.a. Intermediate 1, 17 x 17 cells	75
Figure C.3.1.b. Intermediate 1, 33 x 33 cells	75
Figure C.3.1.c. Intermediate 1, 50 x 50 cells	76
Figure C.3.1.d. Intermediate 1, 67 x 67 cells	76
Figure C.3.1.e. Intermediate 1, 83 x 83 cells	77
Figure C.3.1.f. Intermediate 1, 100 x 100 cells	77
Figure C.3.2.a. Intermediate 2, 17 x 17 cells	78
Figure C.3.2.b. Intermediate 2, 33 x 33 cells	78
Figure C.3.2.c. Intermediate 2, 50 x 50 cells	79
Figure C.3.2.d. Intermediate 2, 67 x 67 cells	79
Figure C.3.2.e. Intermediate 2, 83 x 83 cells	80
Figure C.3.2.f. Intermediate 2, 100 x 100 cells	80

INTRODUCTION

Landscape fragmentation is an inevitable consequence of human alteration of the environment (Forman and Godron 1986). Numerous studies have shown the adverse effects of habitat fragmentation on species behavior (e.g. Wiens and Milne 1989), population levels (e.g. Walker et al. n.d.), biodiversity trends and endemism (e.g. Vergara 1997). Fragmentation threatens the viability of wildlife populations by reducing and isolating habitats, limiting population dispersal and interaction, interfering with host-predator relationships, and causing genetic drift (Walker et al. n.d.).

Fragmentation studies are not limited to wildlife habitats. Young and Jarvis (2001) explored methodology to characterize the physical disruption to the structure of urban landscapes, focusing on the connectivity of areas with different qualities and emphasizing the “adverse effects of urbanization on the connections between quality habitats”.

As long as there are human habitation utilizing resources on landscapes for sustenance, their fragmentation will continue. Understanding the relation of fragmentation patterns and ecological processes is imperative in guiding policy to optimize resource utilization without jeopardizing their sustainability.

However, even after two decades of quantitative landscape ecology (Kronert et al. 2001), fragmentation patterns still cannot be related to ecological processes on the landscape (Wu and Hobbs 2002). Fragmentation indices are necessarily measured over a given area, certainly not at just one point. The indices are thus discrete and may vary with changes to the area it is measured over. On the other hand, fluxes of matter and energy that describe ecological process are of a continuous nature. I argue that this incompatibility between the factors of patterns and processes is the greatest hindrance to

relating them on a landscape, precluding comparisons between sites and/or with other continuous variables and seriously limiting the scope of research that can be conducted.

Aside from new and further development of landscape metrics, Kronert et al. (2001) advocate standardized model parameters for comparison of indicators from different studies. I maintain that this may not be enough, as the fundamental problem, aside from model standardization, is the effects of scale inherent in landscape metrics. Many have attempted to unravel the scaling relations of current landscape indices (e.g. Frohn 1998, Wu et al. 2002) in an effort to resolve the effects of scale, as data may not always be in the appropriate scale for the desired inferences. Knowledge of scaling relations may lend confidence to inferences drawn from data that were scaled up or down. But this research is still a long way from relating landscape patterns and processes. Using the same scale for studies at different sites does not guarantee they can be compared, unless the areas on which the indices are computed were standardized for all sites. But are standardized areas for all sites feasible or even plausible?

I propose a different approach to the same problem. Spatial processes form the bases for methodology in developing a new index and strategies in identifying the areas over which they should be measured. By computing such an index at selected areas or points within the extent of the study, the fragmentation intensity surface could then be generated through spatial interpolation, converting the initially discrete index into a continuous variable over the landscape. With the generated fragmentation intensity surfaces, results between sites would be comparable in the language of surface topology. Relating landscape patterns to continuous processes on the landscape would now be possible, and not just temporal changes over the same site or qualitative studies within a site.

I. Patterns and Processes

Patterns strongly influence ecological processes (Turner 1989). But processes may also affect observed patterns. Walker et al. (2003) describe how social and economic processes influence deforestation patterns in the Amazonian frontier. Arima et al. (unpub.) link deforestation in the Amazon to the spatial process of road building. Understanding the underlying processes is critical in explaining phenomena. Explaining phenomena is the essence of science. The need for landscape pattern methodology has been often voiced, realizing that therein lay the key for understanding the relationships between patterns and processes in landscapes (e.g., O'Neill et al. 1988, Golley 1989, Turner 1990, McGarigal and Marks 1995, Opdam et al. 2002, Wu and Hobbs 2002). Indeed, a major focus of landscape ecology is quantifying relationships between landscape patterns and ecological processes (McGarigal, et al 2002). The future of landscape ecology depends on whether the geographical (pattern) and the ecological (process) approaches in landscape studies can be integrated (Opdam et al. 2002).

Bastian (2001) identifies as the outstanding features of landscape ecology its focus on structures, processes, and changes; spatial and hierarchical aspects; and the complexity of different factors in a landscape. He relegates to geography the essential task of spatial processing and structuring of aggregated and integrative parameters of landscape ecology. Landscape functions are not just a matter of “fluxes of energy, minerals, nutrients, and species between landscape elements” (Forman and Godron 1986), but also how these fluxes relate to human society (Bastian 2001). However, to achieve this view, and thus unify the science of landscape ecology, methodology is

needed to relate anthropogenic activity on a landscape to the consequent ecological and biophysical changes it will induce. Future ecologically sustainable systems will need spatial arrangements that support the required ecological processes on those landscapes (Opdam et al 2002).

II. Landscape fragmentation indices

A landscape is an area of spatial heterogeneity in at least one factor of interest (Turner et al. 2001, Forman 1995). The most basic element in a landscape is the patch or fragment, a surface area that is different in nature or appearance from its surroundings. Perceptions of landscapes and patches are relative to the observer (Wiens and Milne 1989). Thus modelling landscapes and patches are scale dependent.

Landscape indices were developed to quantify patterns in the landscape. They abound in the literature, measuring everything from distribution, area, density, edge, shape, and core area; isolation and proximity; contrast; contagion, interspersion, connectivity, and diversity; etc., and at all levels, from a single patch, to classes of patches, to the whole landscape (McGarigal et al. 2002). Literally hundreds of indices have been proposed to characterize fragments (e.g. O'Neill et al 1988, McGarigal and Marks 1995, and Frohn 1998). Most are single parametered (McGarigal et al. 2002), but a few have multiple parameters (e.g. Hurd et al n.d, Vergara 1997).

Landscape indices have so proliferated that McGarigal et al. (2002) report attempts by others to derive a minimum parsimonious set of independent indices to describe the landscape. No consensus has yet been reached and they conclude that a single parsimonious set may not even exist. Factor analysis by Cain et al. (1997) and

Riitters et al. (1995) find many indices redundant, but agree on factors interpreted as texture, patch perimeter-area scaling (an indicator of patch complexity) and number of attribute types. However, the former did not test for patch density-area scaling (an indicator for patch density), which the later included in their contributory factors. None tested for patch arrangement.

Table 1. Non-redundant univariate landscape fragmentation indices (Riitters et al 1995).

Index	Formulation	Description
Average patch area perimeter-area ratio (PA-1)	$1/m * \sum_{k=1}^m \frac{OE_k}{\sqrt{S_k}}$	PA-1 measures average patch compaction. OE_k is the number of outside edges enclosing patch k and S_k is the area of patch k in pixels.
Shannon contagion (SHCO)	$1 + \frac{\sum_{i=1}^t \sum_{j=1}^t v_{ij} \ln(v_{ij})}{2 \ln(t)}$	SHCO measures image texture. $v_{ij} = A_{ij} / \sum_{i=1}^t \sum_{j=1}^t A_{ij}^2$ for adjacency matrix A (O'Neill et al 1988, Li and Reynolds 1993).
Average normalized area, square model (NASQ)	$1/m * \sum_{k=1}^m \frac{S_k}{16 \cdot OE_k^2}$	NASQ measures average patch shape. OE_k and S_k are as above.
Patch perimeter-area scaling (OCFT)	$1/\beta_2$	β_2 is the estimated slope of regression of $\ln(OC_k)$ on $\ln(S_k)$ for all patches that do not touch the border of the map. OC_k is the number of outside pixels enclosing patch k and S_k is as above.
Number of attribute classes (NTYP)		The number of different kinds of patches there are.

Wu and Hobbs (2002) identify the following as some of the top research topics of landscape ecology in the 21st century: ecological flows in landscape mosaics; causes, processes, and consequences of land use and land cover change; integrating humans and their activities into landscape ecology; and relating landscape metrics to ecological processes. But for all the landscape metrics developed and used in the past

two decades, the technical and ecological understanding of these metrics are still inadequate, and the relation of landscape metrics to ecological processes remains unresolved.

III. Scale

Unfortunately, the geographic concept of scale has contradictory contexts for geography and the other branches of science (Atkinson and Tate 2000). Cartography treats scale strictly as a ratio of map distance to its corresponding distance on the ground. Hence 1:20,000 is a larger scale than 1:5,000,000 in the cartographic sense. However, scale is also equated with the scope of a phenomenon in most other sciences. Analysis in a township, such as would be covered by a 1:20,000 map, is considered of smaller scale in biology, physics, and sociology than would that in a region described by a 1:5,000,000 map. To avoid ambiguity in this study, reference to the direction of the change in scale will be minimized or expounded in reference to its aspects.

Scale may also be taken to mean the level of detail observable (Tate and Atkinson 2001), corresponding to the geographic sense of the word. The higher the scale, the more detail observable, and vice-versa. Moreover, a change in scale may also mean a change in the size of the aggregation area used for computing attributes of the data. Hence, geographically, increasing scale may increase the map-to-ground distance ratio used, increase the amount of detail observable, and/or decrease the area over which data is aggregated, and vice-versa.

Patterns detected in a landscape are a function of scale (Forman and Godron 1986, Levin 1992). The landscape ecology literature (McGarigal et al. 2002, Turner et al 1989, O'Neill et al. 1996) lists only two aspects of scale that affect observations on a landscape, i.e., extent and grain. Extent is the boundary of the study, corresponding to the upper limit of spatial analysis. Grain is the smallest unit of observable space, akin to spatial resolution in raster imagery.

A fundamental difference between how landscape ecologists and geographers perceive and model space is the concept of spatial support. Akin to the kernel in image processing and geographic information science (ESRI 1992), spatial support is the discrete space or spatial unit of aggregation over which a spatial process is considered (Cressie 1993), or the domain over which a geographical variable may be measured (Tate and Atkinson 2001). It may be as small as the grain, as large as the extent, or anywhere in between, and need not be restricted by size, shape, or orientation. Spatial supports may not be mentioned in the landscape ecology literature, but landscape indices necessarily have to be computed over them. And whenever the areas of interest are larger than the grain or smaller than the extent, the support will have to be distinct from either.

IV. The bias of scale

The Merriam-Webster online dictionary defines bias, among others, as:

- 1) deviation of the expected value of a statistical estimate from the quantity it estimates, or
- 2) systematic error introduced into sampling or testing by selecting or encouraging one outcome or answer over others.

The use of “the effect of scale” seems to me as defining the problem by itself, which I find ambiguous. Although a systematic error is the more prevalent definition of bias in statistics, I propose rather to use “the bias of scale” to mean changes induced in the quantification of a spatial index as the scale at which it is being measured is changed, regardless of direction.

Grain and extent influences the numerical results of landscape metrics (Gergel and Turner 2002). Changes in extent affect observations at the edges, and edge effect biases may be controlled systematically or by simply using an extent larger than the area of interest and then clipping off the edges of the resulting image to obtain a smaller extent.

Changes in grain size have a more profound effect on the observed patterns themselves. Details are lost as grain becomes coarser (Turner et al. 1989). Using different grain or raster cell sizes in examining landscape metrics give rise to quantitative differences in the indices (Kronert et al. 2001). Wu et al. (2002) report on the effect of changing grain and extent on landscape metrics, and classified landscape indices into three categories according to their scaling relationships, i.e. predictable, stepwise, or erratic. But, like others have done in the landscape ecology literature (e.g. Frohn 1998, Turner et al. 1989), change in grain sizes were simulated by using a majority filter, aggregating the original data. Doing this avoids the multi-dimensional problems of using satellite imagery from different platforms, where differences in observations may be attributed to differences not only in spatial but also in temporal, radiometric, and spectral resolutions as well.

In the geographical information literature, Dungan (2001) analyzes the effect on vegetation studies of varying remote sensing scales by using products of different spatial resolution from two platforms. However the reference is to a change in support, even if the study acknowledges work by others where remotely sensed data are artificially degraded to study the effects of changing pixel sizes.

The apparent confusion as to which is grain and which is support lies in the fact that grain can be as small as the support. Support size depends on what the area of interest is. Landscape metrics are influenced by spatial support or the size of the area over which they are computed. Observations are affected through changes in aggregation, one aspect of the familiar modifiable areal unit problem or MAUP (Tate and Atkinson 2001). MAUP is the dependence of spatial relations on supports (Cressie 1993), and different approaches for its solution have been suggested. (e.g. Hay et al. 2001).

V. Limitations of the current landscape indices

Most landscape indices are defined discretely (McGarigal and Marks 1995) over an arbitrary spatial support, or use a moving kernel of fixed dimension to derive the supports (Hurd et al. n.d.). Changing the support or kernel size may change the resulting index (Riitters et al. 2000). Hence landscape fragmentation studies are usually limited to a single site, either at one point in time, as most applications in the literature are, or involve changes over a temporal dimension (e.g. Southworth, et al. 2002). The dependence of landscape indices on support or kernel size is precisely what causes the bias, precluding studies across sites or with other continuous data.

Thus we need to “refine landscape metrics to reflect gradient values and allow a more realistic representation of landscape pattern” (Theobald n.d.).

Moreover, all landscape indices in the literature give only an indication of fragmentation. Hurd et al. (n.d.) measure forest fragmentation in six qualitative terms, combinations of two forest continuity levels and three levels of proportion of forests. O’Neill et al. (1996) used three landscape indices (contagion, dominance, and shape complexity) and proposed to measure fragmentation within the three dimensional data space of these indices as the relative distances of a given landscape to landscapes that were totally fragmented and totally intact. Riitters et al. (1996) consider using single-valued indices in describing landscapes the ideal case precisely to avoid multivariate state spaces. Which begs the question: How do we relate fragmentation to any other quantity, and thus provide insight on the relationship of patterns and processes in a landscape, when fragmentation itself can not as yet be quantified?

VI. Statement of problem

There is currently no normalized, single-valued, multi-parameter landscape index that is not biased by at least support size and will measure fragmentation as a continuous spatial process on the landscape. Such limitation precludes comparative landscape fragmentation studies across sites and/or with other biophysical attributes, seriously hampering research and understanding of patterns and processes on the landscape.

VII. Objectives

To relate fragmentation to processes in the landscape, I seek to explore methods to develop an index that describes fragmentation as a continuous phenomenon over the landscape and propose strategies to determine the location and size of the areas over which they should be computed. Specifically, I will:

1. Propose a landscape fragmentation index that describes fragmentation as a spatial process.
2. Derive nested supports of actual landscape scenarios from classified satellite imagery over which the proposed index will be computed to evaluate its ability to describe fragmentation.
3. Explore methods to confirm the bias of grain through regression of the computed landscape indices from two co-registered images of different resolutions against their corresponding supports.
4. Develop methodological frameworks to determine the location of points or supports for generating the landscape fragmentation intensity surface.

VIII. Fragmentation

The landscape fragmentation index discussed here is an improvement of one I proposed (Vergara 1997) to answer the question: “Given two landscapes defined on equal supports, which is more fragmented, and by how much”? I consider patch density, patch arrangement, and patch shape complexity as the essential attributes of fragments to characterize their configuration within an area and thus describe

fragmentation as a spatial process, although I defer defining spatial processes until later.

The landscapes to be analyzed were derived from satellite data classified into binary images of forest-dominated landscapes (represented as 0's) and non-forest fragments (represented as 1's). The raster data model is used throughout. In the discussion, non-forest fragments are synonymous to patches and will be used interchangeably. Index and metric will also be taken to mean the same thing.

A. Patch density, arrangement and shape complexity

To illustrate how the above attributes affect fragmentation, consider three hypothetical landscapes where one of the above parameters is varied while the other two are held constant. First define landscape fragmentation as the breaking up of the original cover, say forest. Fragmentation decreases the areas of contiguous, convex-hull polygons of forested areas, i.e. polygons such that any two points within can only be joined by a line that may touch but does not cross an edge.

For the first case, obviously as the number and/or size of fragments in the landscape increases, so will the proportion of patch pixels to non-patch pixels, increasing fragmentation (Figure 1.1).

The arrangement of patches over a landscape also affects fragmentation. Assume next a landscape with a fixed number of equally sized fragments that can be moved about. Fragmentation decreases as the average distance between patches decreases, i.e. as patch arrangement changes from uniform, to random, to

clustered, and the size of whole and contiguous non-patch areas increases without changing the patch pixel to non-patch pixel ratio (Figure 1.2).

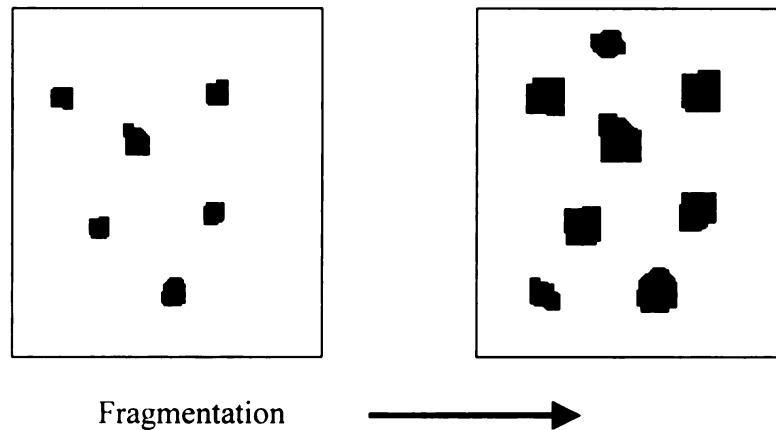


Figure 1.1. Increasing number and sizes of patches

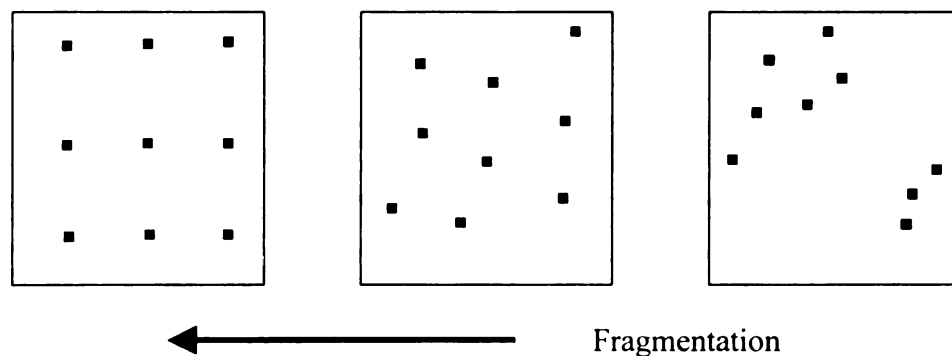


Figure 1.2. Uniform, random, and clustered patches

For the last case, consider a landscape with a single large but pliant patch. Fragmentation increases as patch shape complexity increases, i.e. as the shape of the patch goes from compact or regular to a complex, non-convex hull, and the

size of whole, contiguous, non-patch areas decreases despite constant patch pixel to non-patch pixel ratio (Figure 1.3.).

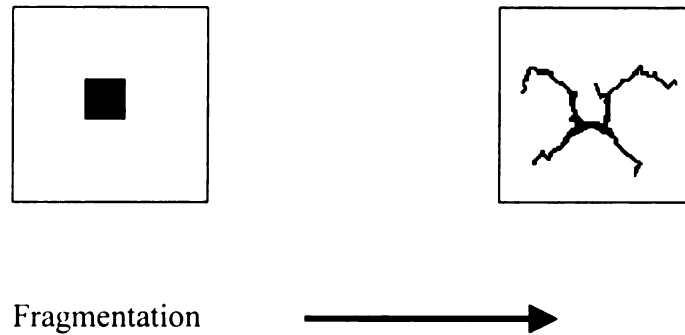


Figure 1.3. Patch shape complexity

From the above illustrations, it should be clear that landscape fragmentation is more intuitively related to the number and size of the patches, rather than to the complexity of their shapes. Shape complexity can increase, increasing fragmentation, without increasing the patch to non-patch pixel ratio. Increasing patch density necessarily increases this ratio, and thus affects fragmentation dramatically.

B. Estimates of index parameters

Patch density

Patch number and size can be estimated by patch density, which is simply the proportion of patch pixels to the total number of pixels in the support. With all else held constant, the higher the patch density, the more fragmentation there is. Patch density is bounded between 0 and 1.

Patch arrangement

The arrangement of patch pixels can be estimated by the quadrat coefficient. Quadrats are equal areal divisions of space. The QUADRAT module of IDRISI assumes the input image contains integer counts in its pixels. It computes the mean number of counts or density per pixel, and the variance in the totals of the counts in the quadrats (Eastman 1996). The quadrat coefficient is the ratio of the quadrat variance to the mean. In binary images, since a pixel can have at most a value of 1 (for patch pixels), the quadrat mean is also the patch pixel density, the proportion of patch pixels to the total number of pixels.

The quadrat coefficient ranges from 0 to 2. Values less than 1 indicate more uniform arrangements, those closer to 1 indicate random arrangements, and those greater than 1 indicate clustering. When the patch density is 1, every pixel in the support is 1 as well, and the quadrat variance will be 0, so the quadrat coefficient is 0. However, when the patch density is 0, the quadrat coefficient is undefined.

Patch shape complexity

Due to limitations in the indices used to measure it, patch shape complexity is the parameter that is most difficult to model. The fractal dimension (de Cola 1989) is one of the earliest indices developed to measure patch shape complexity. Ranging from 1 for regular polygons to values just less than 2 for more complex shapes, it is usually computed as the slope of the regression of the logarithm of the patch perimeters against the logarithm of the square roots of the corresponding patch areas. Issues concerning the fractal dimension include computational as well as conceptual ones (Frohn 1998, Leduc et al. 1994). Firstly, it is impossible

to compute the fractal dimension of a single patch by regression. Secondly, most patches are not true fractals, which should be self-similar at whatever scale they are observed (Mandelbrot 1982) and hence violate an assumption on its application.

Frohn (1998) developed an alternative to the fractal dimension that is more appropriate to the spatial raster data model on which satellite imagery is based:

$$\text{SqP} = 1 - (4 * \text{sqrt}(\text{Area}) / \text{perimeter}).$$

Both area and perimeter are that of pixels and are thus unitless. SqP ranges from 0 for a square, the most compact polygon in a raster model using square pixels (since $4 * \text{sqrt}(\text{area}) = \text{perimeter}$, thus $\text{SqP} = 0$), to values closer to 1 for more complex shapes (where $4 * \text{sqrt}(\text{area}) < \text{perimeter}$, thus $\text{SqP} > 0$). The issues related to the fractal dimension are thus resolved since SqP can now be computed even for a single patch. Neither should there be concern on whether the patches are true fractals since that was never an assumption of SqP.

However, SqP has its own limitations. One issue with SqP is when there is no patch, and both area and perimeter are 0. Will SqP equal 1, corresponding to the most complex shape even if there is none, will it be undefined, or does it go to negative infinity? There are other issues regarding the use of SqP in classifying satellite data (Messina et al n.d.). But the major concern with SqP is the inability to distinguish between a single patch and a group of patches. A simple example should illustrate the point.

Imagine a single, square patch pixel. $\text{SqP} = 1 - (4 * \text{sqrt}(1)/4) = 0$ in this case for the most compact shape in the raster data model. Now imagine four separate

and distinct patch pixels. Logically, SqP should also be 0 since the number of patches should not affect patch shape complexity if the patches have the same shapes. But $SqP = 1 - (4 * \sqrt{4}) / 16 = 1 - (4 * 1/8) = 1 - 1/2 = 1/2$ in this case, which is the shape complexity of a patch polygon composed of four patch pixels joined only at the corners.

But despite this major issue concerning SqP, rather than use two indices for different instances, i.e. either a single or several patches, I will continue to model patch shape complexity with SqP for the work to proceed, until a better alternative is available.

C. Development of the proposed index

As a start, since fragmentation increases with patch density and shape complexity, and decreases as clustering increases, i.e. as the quadrat coefficient increases, the fragmentation index should be of the form of the explicit function below:

$$f = \frac{g(d, SqP)}{h(Q)}, \text{ where } g \text{ and } h \text{ are functions,}$$

with the following assumptions:

f := fragmentation index

d := patch density, $0 \leq d \leq 1$,

SqP := patch shape complexity, $0 \leq SqP \leq 1$, such that $SqP = 1$ if $d = 0$, and $SqP = 0$ if $d = 1$,

Q := quadrat coefficient, $0 \leq Q < 2$, such that $Q = 0$ if $d = 0$ or $d = 1$.

To keep f defined when $Q = 0$, let $h(Q) = 1 + Q$. Let $g(d, \text{SqP}) = d * \text{SqP}$, thus:

$$f = \frac{d * \text{SqP}}{1 + Q}, \text{ such that } 0 \leq f \leq 1$$

since $d \leq 1$, $\text{SqP} \leq 1$, and $1 + Q \geq 1$.

But there is a computational issue involved with this definition. When $d = 0$, i.e. when there is no patch, $Q = 0$ and $\text{SqP} = 1$ by the above assumptions, hence $f = 0$, which is what we want. However, when $d = 1$, i.e. every pixel is a patch pixel, then $\text{SqP} = 0$ and $Q = 0$ again from the above assumptions, and $f = 0$ as well, which is contradictory.

To remedy this, we instead let $g(d, \text{SqP}) = d * (1 + \text{SqP})$, thus:

$$f = \frac{d * (1 + \text{SqP})}{1 + Q},$$

so when $d = 1$, $\text{SqP} = 0$, $Q = 0$, and $f = 1$, which is what we need.

But for d and SqP close to 1, Q could be close to 0 and it is possible that the index will be greater than 1. Hence the numerator must be weighted for the bounds to hold. Since the index is more intuitively related to patch density than to SqP , we let $g(d, \text{SqP}) = d * (1 + (\alpha * \text{SqP}))$ to control the influence of SqP so as to keep f bounded, thus:

$$f = \frac{d * (1 + (\alpha * \text{SqP}))}{1 + Q},$$

such that α is a constant to control the influence of patch shape complexity on the index, and $0 \leq f \leq 1$ holds.

As it is presently defined, the weight on SqP is the most questionable part of this model. But until improved estimates of the parameters are available and definite relationships between them are established, the above model will be used for the purpose of continuity.

IX. Overcoming the bias of spatial support

Assume fragmentation intensity to be continuous over the landscape. Computing the fragmentation index at the critical locations to define the characteristic intensity surface is an essential step in its generation. Although there are methods to derive the surface directly from the binary data, the surface generated in this manner may not be appropriate for analysis, as will be explained below.

A. Smoothing the surface

Raster images of discrete, polygon features can be converted into a surface of continuous values by a number of ways. Image processing and geographical information systems rely on numerical techniques to smooth images of discrete areas or points, such as those for deriving digital elevation models (Eastman 1996). Statistical methods exist for interpolating surfaces from zonal (areal) data (Bailey and Gatrell 1995). Brief descriptions and discussions on their inappropriateness follow.

1. Low pass or mean filter

Generally used in image processing, this technique involves a moving kernel, usually square of odd dimension, over the whole input image,

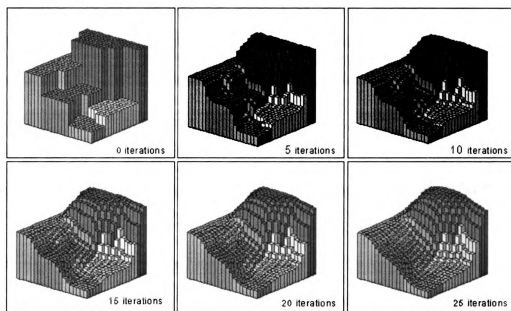
averaging the pixels surrounding the center of the kernel, and assigning the result to the corresponding pixel in the output image (Eastman 1996). The result is an averaged image with smoothed boundaries between discrete polygons. The process is repeated until the desired effect is achieved. This technique is a quick and easy way to handle extreme values in image processing or geographical information systems but would be an inappropriate method for producing the fragmentation intensity surface. The primary issue is the subjectivity in deciding when the desired surface smoothness has been achieved.

2. Pycnophylatic interpolations

This technique smoothens discrete surfaces, such as populations in census tracts, while maintaining the volume under the areas of the original surface (Tobler 1979) and satisfying a non-negativity constraint (Figure 2.). What is taken off one cell is added to another within the same area. Again the technique is applied repeatedly until a number of iterations has been reached or a smoothing requirement satisfied.

However, since the fragmentation data has only 0's and 1's, smoothing the surface in this manner would necessarily produce cells that would be greater than 1 near the centers of the fragment polygons. Moreover, the non-negativity constraint would have to be relaxed to smooth the non-patch areas, and may produce cells that are less than 0. Aside from the arbitrariness of

deciding when to terminate the procedure, interpretation of values greater than 1 or less than 0 would be ambiguous.



Pycnophylactic Interpolation

Figure 2. Pycnophylactic interpolation

Source url: <http://www.ncgia.ucsd.edu/pubs/gdp/pop/pycno.html>*

- note: Original is in color.

3. Kriging

Kriging is a statistical method of spatial interpolation for point, lattice, or zonal (areal) data (Cressie 1993). There are different approaches for handling various data types, and all produce a measure of uncertainty of the predictions. Block kriging is used for zonal or areal data, the closest to thematic images. But the complex, non-convex hull shapes that non-forest fragments may take are not amenable to use as zones in block kriging. Neither do the thematic values of 1's and 0's reflect the true intensity of fragmentation.

B. Spatial processes

To develop the approaches for determining the size and locations of the supports over which to compute the indices to be used in generating the fragmentation intensity surface, the concept of spatial processes must be introduced. A spatial process is a stochastic process operating over a structure of spatial objects. The random, stochastic process defines the relationships between the deterministic spatial objects, as manifested by their current configuration. Observed patterns in a landscape, i.e. the arrangements of spatial objects, are assumed to be random manifestations of the many possible realizations of the hypothesized underlying spatial process (Tiefelsdorf 2000). In our case, the spatial objects are the patch and non-patch pixels, and the supports over which they are observed. All other features (points, lines, and polygons) in a binary raster model of space would have to be defined by the arrangements and states of the pixels within the support. Hence detection of a spatial process is dependent upon the support used as well as the arrangement and values of the pixels contained therein. Spatial processes are not mutually exclusive and several may be operating under any given area being observed, complicating analysis. At present only the most fundamental manner of detecting a spatial process will be explored.

1. Areal approach

By finding the support size when a change in spatial structure is detected, the maximum support encompassing the underlying spatial process may be

determined. Fragmentation is assumed to be homogenous over the support for which a single spatial process was detected, and computing the index over this support assures us that we are free of the pitfalls of the modifiable areal unit problem (Tiefelsdorf 2000). Determining the range of supports where the spatial structure changes then is instrumental, and the search can be applied iteratively to obtain the maximum support just before the change in spatial structure occurs, or until the least non-trivial support size is reached.

2. Point estimation approach

To estimate the fragmentation index at a point or a pixel, a spatial autoregression model over nested supports of increasing sizes centered on that pixel is needed. Although conceptually easy to comprehend, the total dependence of sequential observations would lead to autocorrelation in the observations and/or the residuals. Autocorrelation in the residuals would lead to inaccurate standard errors or invalid inferences (Poole and O'Farrel 1971, Johnston 1978) for ordinary least squares regression. To remedy this, information on the nature of the autocorrelation function is needed. If an autoregressive model could be specified to handle totally dependent observations, the intercept and standard errors at the points already estimated could be used to determine the search radius to the next point. Criteria for determining the spatial arrangement of points to be estimated and used for generating the surface would now exist.

C. Generating the fragmentation intensity surface

Once the fragmentation index has been computed for the determined supports or estimated for a sample of points or pixels, there are again numerical and statistical techniques for generating the surface. By converting the areal data into points through computation of the centroids, the surface could be generated graphically as a digital elevation model or a gravity model (Eastman 1996). However no estimate of accuracy, precision, or uncertainty of the generated surface will be produced.

The surface can also be generated statistically from point data by ordinary kriging on the centroids, or from zone (areal) data by block kriging on the supports, with corresponding estimates of the uncertainty of the results (Bailey and Gatrell 1995). These techniques will not be expounded here as they are beyond the objectives of the study, although it is worth mentioning the compromises in accuracy and precision when generating the fragmentation intensity surface from point or areal data by numerical or statistical interpolation.

MATERIALS AND METHODS

To explore methods that may help confirm the bias of grain on the proposed fragmentation index, two satellite images of the same area acquired as close as possible in time but at different spatial resolutions will be analyzed. Since it has already been established that more detail will be observable with finer grain, and that changes may be due to more than just spatial resolution, it seems reasonable to expect the index to vary for co-incident supports on images of different grain. However, it remains to be seen if the estimates of the fragmentation index for null supports are also affected by changes in grain. In the methodology for overcoming the bias of spatial support, only the ETM+ imagery will be used.

I. Satellite imagery

The satellite images used are ETM+ (30 x 30 m) acquired in 1999 and IKONOS (4 x 4 m) acquired in 2001 of the Legal Amazon in Uruara, Para in Barzil (Figure 3). The images were co-registered and corrected for atmospheric effects. Supervised classification with ERDAS Imagine using all seven bands (including the thermal Band 6) in the ETM+ image produced 14 classes, which were reclassified into five themes: forest, deforested, cloud, shadow, and water. The final classification shows only forest and non-forest classes. Unsupervised classification on the Ikonos image produced at least 40 isodata classes, which were reclassified to the same five themes, then generalized into forest and non-forest classes as well.

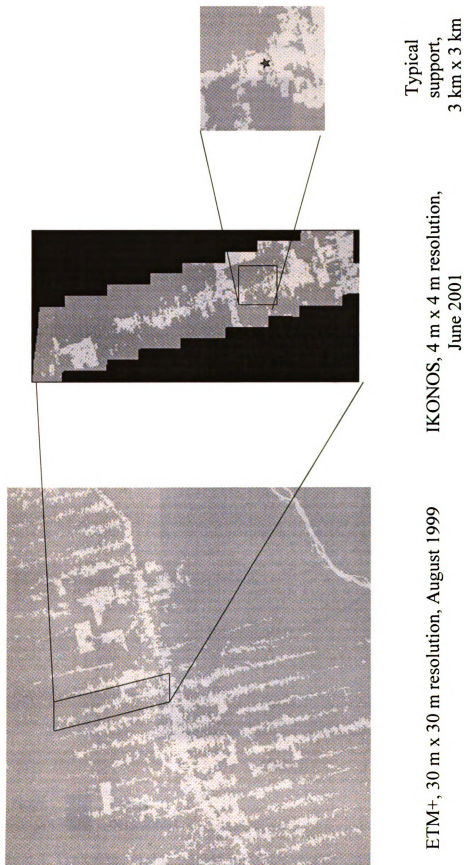


Figure 3. Satellite imagery showing forest fragmentation at different resolutions, Uruara, Para in the Legal Amazon.

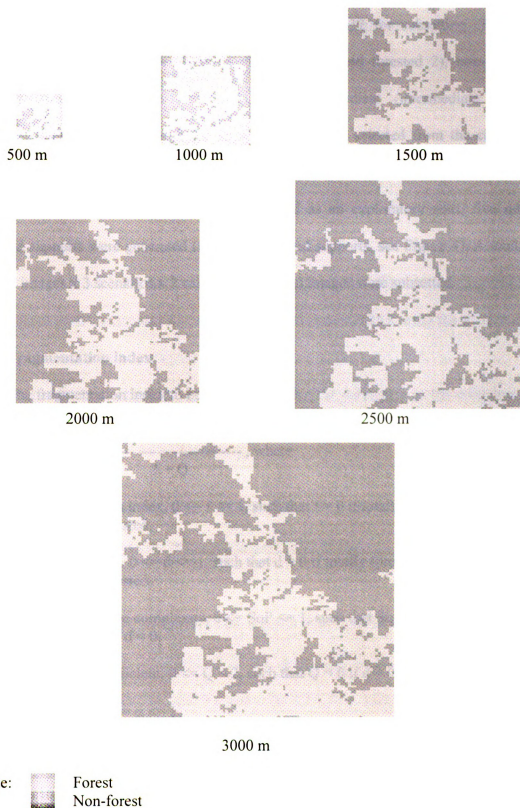


Figure 4. Typical increasing support for fragmentation study

II. Nested supports

The classified images were imported into IDRISI32 for subsetting. Two co-incident cases each of forest-dominated (forested 1 and forested 2), non-forested (non-forested 1 and non-forested 2), and intermediate (intermediate 1 and intermediate 2) scenarios with the least variation were selected from the classified ETM+ and Ikonos imagery. The maximum support common to all areas without going beyond the extents was determined, and as an exploratory start, five other nested supports were generated (for typical nested supports, see Figure 4). A total of 72 (2 images x 3 scenarios x 2 cases x 6 supports) images were subsetting.

III. Fragmentation index

The fragmentation index to be used is:

$$f = \frac{d * (1 + (\alpha * SqP))}{1 + Q}, \text{ where}$$

f := fragmentation index, $0 \leq f \leq 1$, such that $f = 0$ if totally forested and $f = 1$ if totally deforested,

d := patch density, $0 \leq d \leq 1$, such that $d = 0$ if totally forested and $d = 1$ if totally deforested,

SqP := patch shape complexity, $0 \leq SqP \leq 1$, such that $SqP = 1$ if $d = 0$, and $SqP = 0$ if $d = 1$,

Q := quadrat coefficient, $0 \leq Q < 2$, such that $Q = 0$ if $d = 0$ or $d = 1$, and

α := constant, $0 \leq \alpha \leq 1$.

The index was computed on the determined supports using six values for α (0, 1, 0.25, 0.125, 0.01, and 0.001) and the effect of α on the index was noted. The total

patch area, total patch perimeter, quadrat coefficient, and patch density were derived in IDRISI32 for all 72 supports. SqP and the fragmentation index were computed in Windows Excel.

IV. Variograms and first lag gammas

Variograms are devices used to explore spatial dependence or the second order properties in a spatial process (Bailey and Gatrell 1995). The subsetting, classified ETM+ images were converted into ASCII vectors of 0's and 1's and turned into spatial point process objects in S+. Variograms (formally called semi-variogram) for the lagged pixel distances were computed, plotted and modelled using the exponential variogram model with an emphasis on the front end of the variogram.

Theoretically, Bailey and Gatrell (1995) define the variogram as the difference in the variance and covariance due to distance \mathbf{h} as:

$$\gamma(\mathbf{h}) = \sigma^2 - C(\mathbf{h}),$$

where $\mathbf{h} = \mathbf{s}_i - \mathbf{s}_j$ is the vector difference between \mathbf{s}_i and \mathbf{s}_j for a spatial stochastic process $Y(\mathbf{s})$ with variance $\sigma^2(\mathbf{s})$, mean $\mu(\mathbf{s})$, and covariance $C(\mathbf{h})$ due only to the distance \mathbf{h} , thus:

$$C(\mathbf{h}) = C(\mathbf{s}_i - \mathbf{s}_j) = C(\mathbf{s}_i, \mathbf{s}_j) = E((Y(\mathbf{s}_i) - \mu(\mathbf{s}_i))(Y(\mathbf{s}_j) - \mu(\mathbf{s}_j))).$$

A spatial process is stationary if the mean and variance are constant and independent of location, i.e., $\mu(\mathbf{s}) = \mu$ and $\sigma^2(\mathbf{s}) = \sigma^2$. The variogram model assumes a stationary process. If first order or global trends do not affect a spatial process, variance levels off as distance between point pairs increases. The maximum variance that the variogram model reaches is called the sill. The distance between pixels where

the variogram model reaches its sill is defined as the range, the maximum distance up to where spatial dependence manifests, beyond which the spatial objects are independent, and the variogram model is flat in that region as it approaches an asymptote (Figure 5).

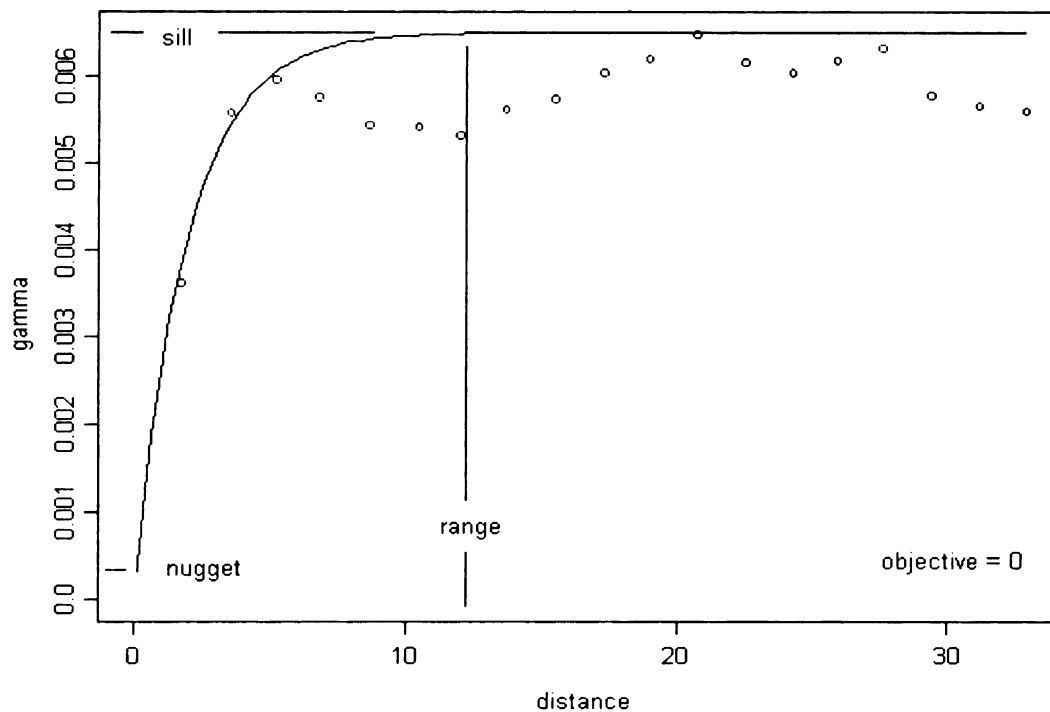


Figure 5. Typical variogram and exponential model showing nugget, sill and range variances.

The variogram model starts at its nugget, which ideally should be 0. When it is not, there may be sampling errors or variability in the very shortest distances that the model cannot account for. The behavior of the range, the first lagged gamma values, and the overall variances over the changing supports were plotted, summarized, and explored, with the aim of determining if these could be used to indicate a change in spatial structure.

An absence of spatial dependence in a spatial process, as what would happen within a totally forested or deforested support, would result in a flat variogram, referred to as a pure nugget model. A change from a pure nugget model to one that has a range and sill indicates a change in spatial structure, hence a change in spatial process. A variogram that is not pure nugget but has no apparent sill or range is unbounded, with spatial dependence increasing with distance between pixels.

V. Autocorrelation

The spatial point process objects of 0's and 1's from the classified ETM+ images were converted into lattices, and Moran's I and Geary's C based on 1000 permutations (Kaluzny et al. 1997) were computed using the 8 nearest equally weighted neighbors. The king's case with equal weights includes normal as well as diagonal joins and thus equally considers adjacent pixels in any direction. Moran's I and Geary's C were tested over the number of permutations for statistical difference from a random arrangement of the pixels in a support. The change in statistical significance of the measures of spatial autocorrelation was used as an indicator of a change in spatial structure as support size changed.

VI. Regressions

The fragmentation index at different α levels over the supports from the ETM+ and Ikonos images were evaluated, and an α was chosen for the regression. The computed indices were regressed against the absolute areas of the corresponding supports using ordinary least squares (OLS). As an exploratory start to confirm the

bias of grain size, the slope and intercept estimates of the two images for all cases were compared. If the estimates of one image are within the bounds of the standard errors of the corresponding case of the other image, this line of investigation may be worth looking into in more depth.

RESULTS AND DISCUSSION

I. Fragmentation index

At $\alpha = 1, 0.25$, and 0.125 , the fragmentation indices were greater than 1 for some of the non-forested and intermediate cases, notably for the smaller supports (Table A.2.a, Table A.2.b, and Table A.3.a in Appendix A). The influence of patch shape complexity to the index in these cases was excessive. At $\alpha = 0$, patch shape complexity is not considered, i.e., $f = d / (1 + Q)$, and the resulting index intuitively corresponds to patch density, such that there seems to be as much fragmentation as patch density indicates (Tables A.1.a to Table A.3.b in Appendix A). However at this α level the index can not distinguish between the smallest supports of the two non-forested cases (Figures 6.1 and 6.2), which have one patch each, equal numbers of patch and non-patch pixels (113 and 6, respectively) albeit arranged differently, and equal fragmentation indices ($f = 0.959255$ at $\alpha = 0$).

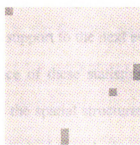


Figure 6.1. Non-forested 1, 17x17 pixels
 $f = 0.959255$ at $\alpha = 0$
 $f = 0.964148$ at $\alpha = 0.01$
 $f = 0.959744$ at $\alpha = 0.001$

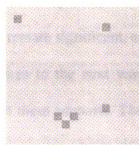



Figure 6.2. Non-forested 2, 17x17 pixels
 $f = 0.959255$ at $\alpha = 0$
 $f = 0.961831$ at $\alpha = 0.01$
 $f = 0.959512$ at $\alpha = 0.001$

Note:  Forest
Non-forest

At $\alpha = 0.01$, this deficiency is resolved and the index identifies the support with more contiguous non-patch pixels as less fragmented ($f = 0.961831$) than the other ($f = 0.964148$). Limiting the value of α to 0.01 affects only the second significant figure of the index, thus $0 \leq f \leq 1$ holds for the current cases and supports. At $\alpha = 0.001$, at most only the third significant figure of the index is affected, and going by patch density alone, $0 \leq f \leq 1$ should hold for all cases and supports smaller than or equal to 100×100 pixels. The index is again intuitively akin to patch density yet differences in spatial arrangement of the fragments are discernable, while still being bound between 0 and 1 (Table A.1.a to Table A.3.b in Appendix A).

II. **Moran's I and Geary's C**

Moran's I and Geary's C, computed over the closest 8 neighbors in a particular support, should give a measure of how similar adjacent pixels are in that support. However, what matters are not the values per se, but detecting changes in their significance. Although the spatial structure and hence the spatial process may change from one support to the next even if these statistics remain significant, a change in the significance of these statistics from one support size to the next would indicate a change in the spatial structures encompassed within these supports. The interest is in the first such detected change, and the two supports at which this change was detected. Performing this test iteratively, it should be possible to determine the maximum support that encompasses a particular spatial process.

In the forested cases (Figure B.1.a and Figure B.1.b in Appendix B), both Moran's I and Geary's C are not significant for the first two supports, but are

significant for the remaining four supports. The spatial structure thus changed significantly between the second and third supports, and it is in that range of supports that an iterative search should be performed. In the non-forested cases (Figure B.2.a and Figure B.2.b in Appendix B), Moran's I and Geary's C are not significant for the first support, and significant for the rest. Hence the change in spatial structure occurred between the first and second support. Moran's I and Geary's C are significant for all supports in the intermediate cases (Figure B.3.a and Figure B.3.b in Appendix B). The support should hence be further reduced until a change in the significance of the autocorrelation measures is detected or the support reaches the minimum, non-trivial case of 3 x 3 pixels where the search terminates.

III. Variogram modelling

Changes in the variogram model from one support to the next could verify changes in the spatial structure encompassed by succeeding supports. A change from a pure nugget model to one with definite structure indicates that a change in spatial structure. In the forested cases, this occurs between the second and third supports (Figure C.1.1.b and Figure C.1.1.c; Figure C.1.2.b, and Figure C.1.2.c in Appendix C), which correspond with the results from the spatial autocorrelation measures. In the non-forested cases, the change in the structure of the variogram model occurs between the first and second supports (Figure C.2.1.a and C.2.1.b; Figure C.2.2.a and Figure C.2.2.b in Appendix C), again corresponding with the results from the spatial autocorrelation measures. For the intermediate cases, the variograms for all supports show definite unbounded structure from the start (Figure C.3.1.a to Figure C.3.2.f in

Appendix C), and so a change in spatial structure cannot be concluded. So as in the previous discussion, the supports should be further reduced, until a change is detected or the minimum, non-trivial support size is reached.

The first lag gammas are the difference between the overall variance and the covariance of adjacent pixels due to distance. If this value is low, then almost all the variance in the spatial process can be explained by adjacent pixel covariance due to distance. Plotting the first lag gammas for the six cases against support size (Figure 7.1) does not show any hint for use as an indicator of change in spatial structure as support changes for all cases. Likewise, neither does the ratio of the first lag gammas to overall variance (Figure 7.2).

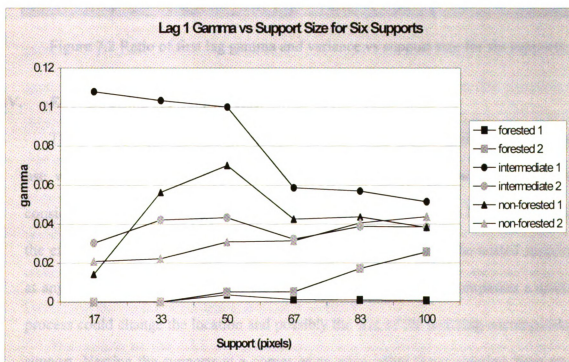


Figure 7.1 First lag gamma and support size for six supports.

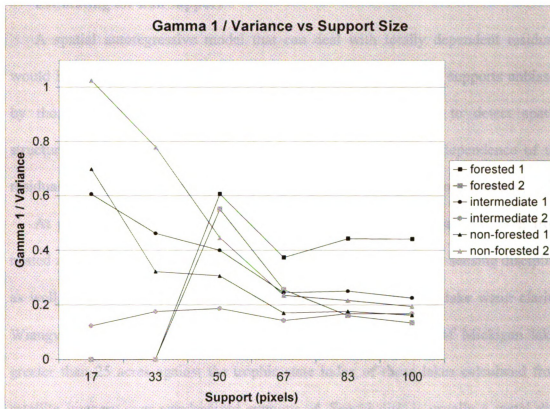


Figure 7.2 Ratio of first lag gamma and variance vs support size for six supports.

IV. Encompassing spatial processes

The methodology outlined above now forms basis for choosing the support size to use when computing the fragmentation index. Support shape and orientation are considered as well since only square supports were used. All that is left to consider is the effect of locating the supports. Due to edge effects, centering the nested supports at any other point or pixel within the determined support that encompasses a spatial process could change the location and possibly the size of the resulting encompassing support. Nesting the supports at a corner or an edge rather than centering them on a pixel would also affect the location of the encompassing support.

V. Estimating for null support

A spatial autoregressive model that can deal with totally dependent residuals would be the ultimate method of rendering indices computed over supports unbiased by those supports. Tiefelsdorf (2000) describes methodology to detect spatial structure by analyzing the spatial autocorrelation of the partial dependence of the residuals of a spatial autoregressive model over non-overlapping zones or areas.

At present there is no autoregressive model to handle observations taken from nested zones or areas. Such a model would be helpful in the remote sensing discipline as well. As an example, to develop methodology for monitoring lake water clarity, Wiangwang (2002) regressed Secchi disk depth measurements of Michigan lakes greater than 25 acres against the trophic state index of those lakes calculated from satellite imagery over standardized supports. A Secchi disk is usually a metal disk painted black and white on alternating quadrants and attached to the end of a graduated tape or cord used to measure turbidity in the water column. The Secchi disk depth is the recorded water depth where the lowered disk just disappears from view. For known sampling locations with global positioning system (GPS) coordinates, a support of 15 pixels centered on the GPS fixes was used. Larger supports of up to 100 pixels were used for the deepest part of the lake where there were no GPS fixes. If a nested spatial autoregression model can be specified, then there would be basis for estimating the trophic state index at a point or pixel.

The results of the OLS regressions over the supports from the two images of different resolutions show that none of the forested intercept estimates are significant (Table 2). The reason may be that the regression was conducted for all six supports,

even if the preceding discussions show that the maximum support size should be between the second and the third supports. The results may have been different if the analysis were conducted over supports with the maximum somewhere between the second and the third supports. In other words, the results from the autocorrelation and variogram analysis would have been useful in identifying the supports over which to conduct the regressions.

Of the remaining intercept estimates only one (non-forested 1) falls within the bounds of their corresponding standard errors. All had equal corresponding signs for their slope estimates. Except for one forested and one intermediate case, the slope and intercept estimates and standard errors aren't that far off. But it is inconclusive whether they are significantly different or not. A two-way (resolution x case) ANOVA test with two sub-samples each for six supports and four statistics (intercept estimate and standard error, and slope estimate and standard error) will suffer from very low degrees of freedom since only 12 observations can be used for each test. Even if a three-way (resolution x case x support) ANOVA test for statistical significance using all 72 observations shows that support as well as grain matters in the cases presented, it will not be enough to conclude that the proposed index is or is not affected by changes in grain. Hence the bias of the index due to grain cannot be confirmed as yet.

Table 2. Summarized slope and intercept estimates with standard errors.

	ETM+		Ikonos	
forested 1	estimate	std error	estimate	std error
intercept	0.000931	0.000824	0.0001162	8.258E-05
slope	4.11E-07	1.69E-06	*6.08E-07	*1.69E-07
	ETM+		Ikonos	
forested 2	estimate	std error	estimate	std error
intercept	-0.024683	0.015486	-0.021611	0.0138089
slope	*0.000165	*0.000031	*0.000139	*0.000028
	ETM+		Ikonos	
Intermediate 1	estimate	std error	estimate	std error
intercept	*0.518843	*0.064561	*0.256548	*0.020722
slope	*-0.00043	*0.000132	*-0.00014	*0.000042
	ETM+		Ikonos	
Intermediate 2	estimate	std error	estimate	std error
intercept	*0.252256	*0.012867	*0.213569	*0.011228
slope	-5.096E-05	2.643E-05	-4.762E-05	2.3066E-05
	ETM+		Ikonos	
non-forested 1	estimate	std error	estimate	std error
intercept	*0.755530	*0.099767	*0.733656	*0.079684
slope	*-0.00069	*0.000204	*-0.00066	*0.000163
	ETM+		Ikonos	
non-forested 2	estimate	std error	estimate	std error
intercept	*0.978665	*0.015969	*1.018715	*0.016883
slope	*-0.00056	*0.000032	*-0.00059	*0.000034

CONCLUSIONS

The proposed index as defined so far was developed to provide a normalized, intuitive measure of landscape fragmentation capable of discerning differences due to patch density, patch arrangement, and patch shape complexity as the necessary conditions to define fragmentation as a spatial process. To maintain the bounds, the estimate for patch shape complexity was weighted to control its influence on the index as the parameter in the numerator with supposedly lesser contribution to fragmentation. This approach does seem arbitrary and since it was tested only for one site with a particular fragmentation pattern, it arguably may not be applicable for other sites with different fragmentation patterns.

The emphasis here is on the methodology to develop the index and render it unbiased by at least support size, not on the index itself. Further research on both natural and synthetic landscapes preferably with improved estimates for patch shape complexity would still be needed to verify the applicability of the weights or uncover the actual relations between the estimates of the parameters of fragmentation. Be that as it may, at least for this site an index to directly quantify fragmentation of binary landscapes is now available.

The methodology to make the fragmentation index unbiased by the size of the spatial support is independent of the index itself. This means that if such methodology could be developed, any index computed over a spatial support that intends to measure an attribute of the encompassed spatial process may be made unbiased by support size using the methodology outlined above. The application of such methodology would be a tremendous help in landscape ecology. Firstly, the generated fragmentation intensity

surfaces of two different sites would now be comparable in the language of surface topology of cusps, manifolds, attractors, singularities, bifurcations, etc., as long as the scale of analysis are roughly equal. Secondly, since biophysical processes on the landscape are assumed to be continuous, their surfaces may also be interpolated from sample data and compared to the generated fragmentation intensity surface, thus providing a framework for relating patterns and processes on the landscape.

The preceding discussions outline methodology to detect a change in spatial structure from one nested support to the next to determine the maximum support that encompasses a spatial process, over which the fragmentation index is computed. The detection of changes in spatial structure from the numerical results of the spatial autocorrelation statistics corresponds to the graphical results from variogram modeling, and though the methodology as developed so far may be elementary, it is nonetheless fundamental. It is however possible that the spatial process may change between two supports but still be indiscernible by the methodology presented. Further research into other indicators of changes in spatial processes for such cases is thus needed. But despite this shortcoming, the choice of support over which to compute the fragmentation index now has basis and need not be arbitrary. The next concern then would be generating the fragmentation intensity surface.

I. Areal approach

Methodology to determine the maximum support encompassing a spatial process (over which to compute the fragmentation index) has been outlined above. But defining a tessellation of the extent, i.e. non-overlapping supports to cover the entire

extent (Tiefelsdorf 2000), that is not prone to the complications of the modifiable areal unit problem due to the bias of location of supports that the methodology as so far described introduces, is another matter. The size and arrangement of the supports for the same image may vary for every solution, as would the generated fragmentation intensity surfaces. The generated surfaces will agree in general structure but may have local variations. Thus the areal approach as outlined above will at best be only heuristic.

A better strategy would be to predetermine the points or pixels at which the supports should be located. Most GIS or image processing applications are capable of distinguishing polygons greater than eight pixels without diagonal joins. The centroids can then be found, even if they lie outside the bounds of the polygon, at which point the search for the appropriate support begins, using center-nested supports. Then the search shifts to a corner of the determined support over the centroid, and using edge or corner nested supports, the process continues along all edges and corners of the first determined support. The search continues to the external supports until the polygon is covered fully by non-overlapping supports. Smaller supports would thus cover the areas closer to the edges of the polygons, with larger supports elsewhere (Figure 8). Doing this for all patches should cover the points of interest within the extent. All that would be left are the areas with no patches or those with patches less than nine pixels. Again the centroids are found for these areas and appropriate supports determined. Even if all the supports do not cover the whole extent edge to edge, all areas of interest would still be considered.

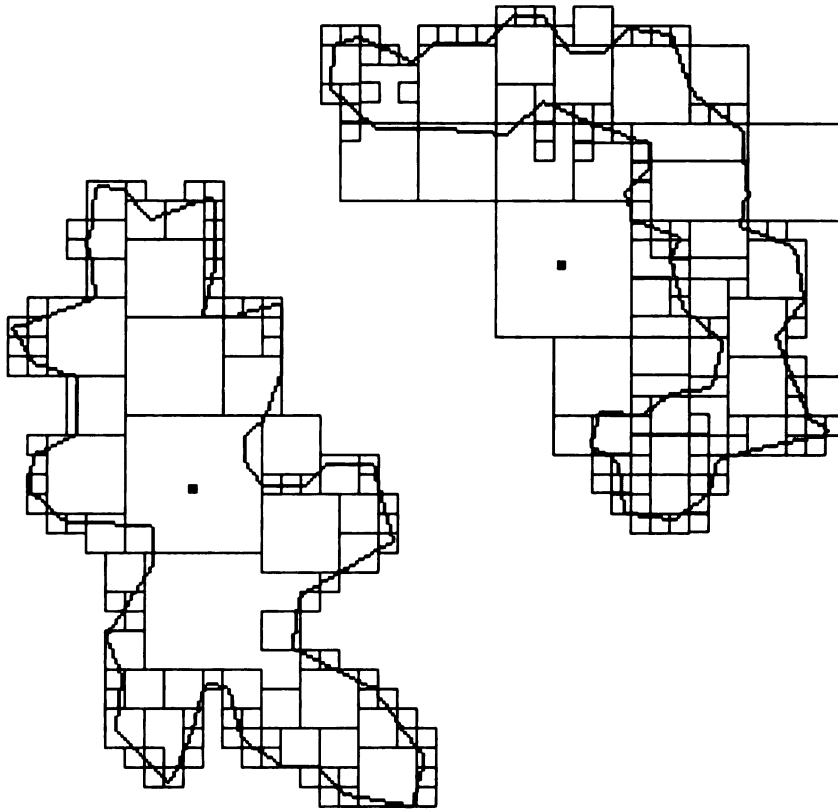


Figure 8. Typical areal estimation.

A better strategy for this approach is to pre-determine not only the areas of interest, i.e. the patch polygons, but also the points at which to generate the surface. A brief digression into elementary graph theory is needed here before the next procedure can be expounded.

A graph is a set of vertices (or points) and edges (or lines) connecting any two vertices, regardless of length, shape or manner of join (Matousek and Nesetril 1998). A path is a trace of edges joining any two vertices. A graph is connected if a path exists for every pair of vertices in the graph. A cycle is a path traversing all vertices

once and returning to the starting vertex. A tree is a connected graph with no cycles. There exists exactly one path for any two vertices on a tree. A spanning tree of a graph is a sub-graph that contains all the vertices of the original graph. A minimum spanning tree is a spanning tree with weighted edges such that the sum of the edges is a minimum.

Hence all polygons are cyclic graphs. The vertices that define the polygon are searched for and a minimum spanning tree with distance-weighted edges wholly circumscribed within the polygon is then derived (Figures 9.1 to 9.4). The difference in the definition above is the liberty of locating the vertices of the minimum spanning tree. The solution should be unique if derived in this manner, although this is postulated and stated here without proof. The vertices of the polygon and the minimum spanning tree are precisely the points to use in generating the surface, for which the appropriate supports would be determined, over which the corresponding indices computed.

II. Point estimation approach

Conceptually the ultimate approach to remedy the bias of support, it is computational imprecise at this point until a spatial autoregression model is specified that could handle observations taken from nested zones or areas. But if such a model could be specified, there should be no ambiguity in determining the location of points to be estimated, given each estimate has a measure of uncertainty. Using the standard error of the intercept and the corresponding slope estimate of the regression line, a pixel radius could be computed for every estimated point. By starting at a corner and

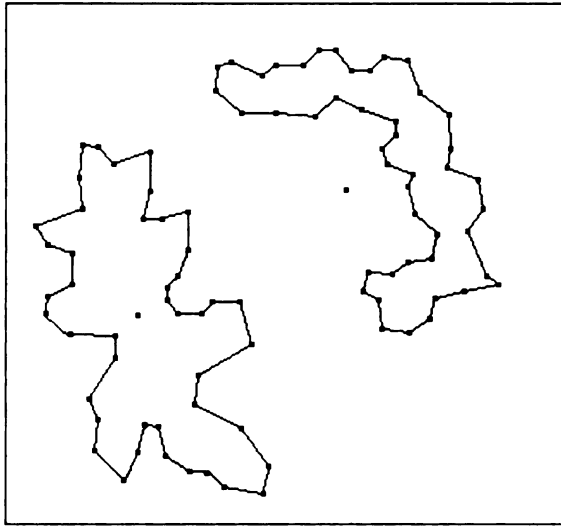


Figure 9.1. Non-convex hull polygons with centroids and vertices.

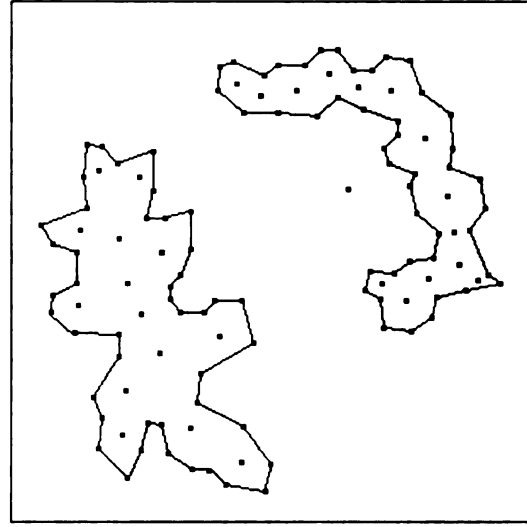


Figure 9.2. Internal vertices determined for spanning tree.

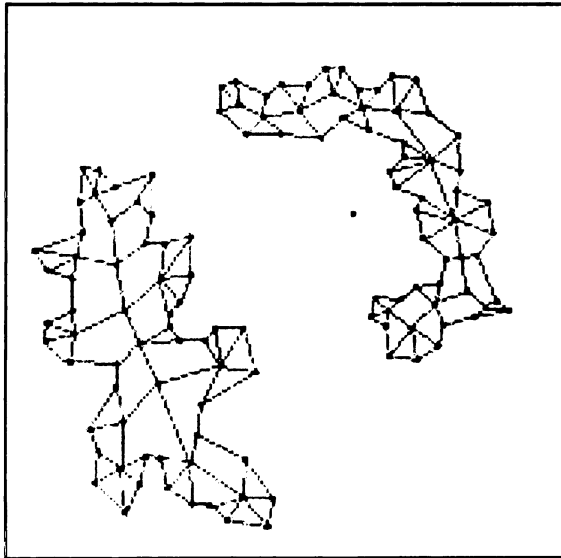


Figure 9.3. Typical spanning tree within the polygon.

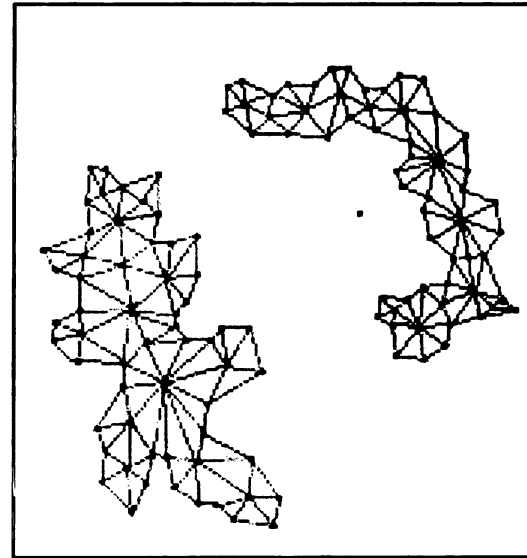


Figure 9.4. Thiessen triangles for surface generation.

using the computed radius to locate the next point along an edge, selected points along all edges could be iteratively located. And just as a jigsaw puzzle is solved after the edges are determined, the internal points are determined next until the whole

extent is covered from the edges to the center. Following this procedure will result in smaller search disks near the edges of the polygon and hence more points to generate the surface, and larger search disks and hence less points elsewhere (Figure 10).

With a lattice of points now determined, the surface can be generated as a digital elevation model (DEM) or by kriging. The arrangement of points may be over-specified for the DEM, and thus be non-optimal, but each point would have an estimate of uncertainty from which the integrity of the generated surface may be gleaned. Kriging would also generate the surface with corresponding estimates of uncertainty as well. Either result might not be distinguishable from the other, given the extensiveness of the sample points from which to generate the surface.

However, since the point samples will be over-specified anyway, there really is no compunction in using the OLS estimates for the points. The true estimates won't be that far off, just that the standard errors may be too optimistic. But an over-specified sample of points could compensate for the loss of precision in the standard errors.

Still the best solution would be to pre-determine the points for generating the surface, as in the previous discussion of finding the minimum spanning tree, and then estimate the fragmentation index at those points using nested spatial autoregression. Done this way, the configuration of the points for surface generation should be optimal, although again this is postulated and stated here without proof.

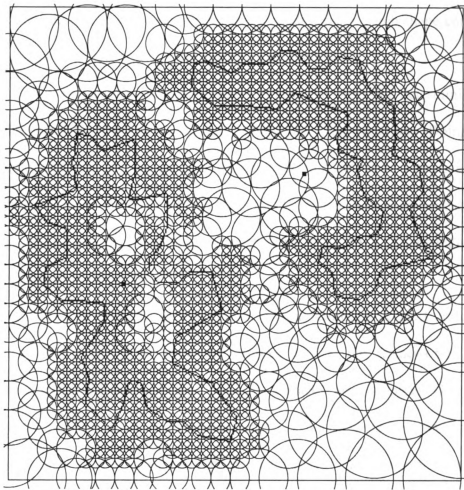


Figure 10. Typical point estimation

RECOMMENDATIONS

A multi-parametered, single-valued, normalized landscape fragmentation index is proposed that can discern differences in patch density, patch shape complexity and patch arrangement and describe fragmentation intuitively.

The underlying spatial processes is now the basis for determining the size of the supports to use in calculating landscape fragmentation. Doing so avoids the complications due to the modifiable areal unit problem. Generating the continuous fragmentation intensity surface from the computed indices encompassing single spatial processes on the determined supports will result in a fragmentation intensity value anywhere in the extent.

Although computationally intensive and requiring at least thrice the amount of computer memory to store the original image, the frameworks outlined here for generating the fragmentation intensity surfaces are tractable. The methodology was developed for forest fragmentation analysis, but it should be applicable to any binary landscape, such as urban and non-urban areas, agricultural and non-agricultural sites, etc. Four major issues remaining are:

1. The availability of better estimates of patch shape complexity to improve the model and determination of their relationships,
2. Specifying a nested spatial autoregression model that can handle totally dependent observations,
3. Confirming the uniqueness of the solution for the minimum spanning tree given any polygon, and

4. Optimizing the search for the vertices of the minimum spanning tree at which to compute the indices and generate the fragmentation intensity surface.

There are other fundamental issues as well. Three parameters necessary to characterize landscape fragmentation were identified, i.e. patch density, patch shape complexity, and patch arrangement. Are they the sufficient conditions as well? If so, then the model may be treated as a mathematical function, and if continuous over a range, the inverse may exist. Identifying the necessary and sufficient conditions of a functional relationship lends confidence to the inferences that may be drawn by using them. Moreover, verifying that the inverse function exists paves way for further research into its applicability. Is $1 - f$ the fragmentation index for the non-patch pixels?

For now, these are the only parameters that come to mind, although that gives no assurance that they are the only ones. Future research may help to identify other factors that characterize fragmentation in the landscape, or confirm that these indeed are necessary as well as sufficient.

The appropriateness of the estimates of the model parameters may also be questioned. Does the quadrat coefficient really measure patch arrangement? Is SqP the best estimator for patch shape complexity? For now these are what are available, and the model would definitely benefit from improved parameter estimates subject to their availability.

Lastly the assignment of the weight for SqP may also be scrutinized as arbitrary. The parameters to characterize landscape fragmentation are inter-related, and more work is required to determine their relationships. The assignment of $\alpha = 0.001$ may work for the current configuration, as only one fragmentation pattern was analyzed. Will it hold for

other regions as well, even if the anthropogenic view of the world with its corresponding scale is maintained?

As an exploratory first step, this research elicits more questions than answers. But such is the nature of exploration, hence the title of this research. I hope I have stirred enough interest to warrant more research along these lines of scholarship.

APPENDICES

APPENDIX A

Summaries for Fragmentation Parameters and Indices

Table A.1.a. Forested 1

$$f = (d * (1 + (a * SqP)))/(1+Q)$$

etm+					a = 0	a = 1	a = 0.25	a = .125	a=0.01	a = .001
	n	d	Q	SqP	f0	f1	f2	f3	f4	f5
1	289	0.00000	0.00000	0.00000	0.00000	0.00000	0.00000	0.00000	0.00000	0.00000
2	1089	0.00000	0.00000	0.00000	0.00000	0.00000	0.00000	0.00000	0.00000	0.00000
3	2500	0.00600	0.99440	0.29582	0.00301	0.00390	0.00323	0.00312	0.00302	0.00301
4	4489	0.00334	0.99688	0.29582	0.00167	0.00217	0.00180	0.00174	0.00168	0.00167
5	6889	0.00218	0.99797	0.29582	0.00109	0.00141	0.00117	0.00113	0.00109	0.00109
6	10000	0.00150	0.99860	0.29582	0.00075	0.00097	0.00081	0.00078	0.00075	0.00075

ikonos					a = 0	a = 1	a = 0.25	a = .125	a=0.01	a = .001
	n	d	Q	SqP	f0	f1	f2	f3	f4	f5
1	15625	0.00000	0.00000	0.00000	0.00000	0.00000	0.00000	0.00000	0.00000	0.00000
2	62500	0.00032	0.99970	0.52925	0.00016	0.00024	0.00018	0.00017	0.00016	0.00016
3	140625	0.00067	0.99934	0.80989	0.00033	0.00060	0.00040	0.00037	0.00034	0.00033
4	250000	0.00108	0.99892	0.88071	0.00054	0.00102	0.00066	0.00060	0.00055	0.00054
5	390625	0.00087	0.99914	0.89786	0.00043	0.00082	0.00053	0.00048	0.00044	0.00043
6	562500	0.00122	0.99878	0.92764	0.00061	0.00118	0.00075	0.00068	0.00062	0.00061

Table A.1.b. Forested 2

$$f = (d * (1 + (a * SqP)))/(1+Q)$$

etm+					a = 0	a = 1	a = 0.25	a = .125	a=0.01	a = .001
	n	d	Q	SqP	f0	f1	f2	f3	f4	f5
1	289	0.00000	0.00000	0.00000	0.00000	0.00000	0.00000	0.00000	0.00000	0.00000
2	1089	0.00000	0.00000	0.00000	0.00000	0.00000	0.00000	0.00000	0.00000	0.00000
3	2500	0.00920	0.99120	0.49518	0.00462	0.00691	0.00519	0.00491	0.00464	0.00462
4	4422	0.02058	0.97964	0.65931	0.01040	0.01725	0.01211	0.01125	0.01046	0.01040
5	6972	0.12134	0.87878	0.78923	0.06459	0.11556	0.07733	0.07096	0.06510	0.06464
6	10000	0.25710	0.74297	0.82019	0.14751	0.26849	0.17775	0.16263	0.14872	0.14763

ikonos					a = 0	a = 1	a = 0.25	a = .125	a=0.01	a = .001
	n	d	Q	SqP	f0	f1	f2	f3	f4	f5
1	15625	0.00000	0.00000	0.00000	0.00000	0.00000	0.00000	0.00000	0.00000	0.00000
2	62500	0.00034	0.99968	0.54174	0.00017	0.00026	0.00019	0.00018	0.00017	0.00017
3	140625	0.00399	0.99602	0.85985	0.00200	0.00372	0.00243	0.00221	0.00202	0.00200
4	250000	0.01536	0.98464	0.91569	0.00774	0.01483	0.00951	0.00863	0.00781	0.00775
5	390625	0.09863	0.90137	0.93002	0.05188	0.10012	0.06394	0.05791	0.05236	0.05192
6	562500	0.22280	0.77720	0.94452	0.12537	0.24378	0.15497	0.14017	0.12655	0.12549

Table A.2.a. Non-forested 1

$$f = (d * (1 + (a * \text{SqP}))) / (1 + Q)$$

etm+										
	n	d	Q	SqP	a = 0 f0	a = 1 f1	a = 0.25 f2	a = .125 f3	a = 0.01 f4	a = .001 f5
1	289	0.97924	0.02083	0.51010	0.95925	1.44857	1.08158	1.02042	0.96415	0.95974
2	1089	0.77502	0.22518	0.75350	0.63258	1.10923	0.75174	0.69216	0.63734	0.63305
3	2500	0.64640	0.35374	0.78377	0.47749	0.85173	0.57105	0.52427	0.48123	0.47787
4	4489	0.52439	0.47571	0.80380	0.35535	0.64098	0.42676	0.39105	0.35821	0.35563
5	6889	0.44491	0.55517	0.80298	0.28609	0.51581	0.34352	0.31480	0.28838	0.28632
6	10000	0.38190	0.61816	0.82343	0.23601	0.43035	0.28459	0.26030	0.23795	0.23620

ikonos										
	n	d	Q	SqP	a = 0 f0	a = 1 f1	a = 0.25 f2	a = .125 f3	a = 0.01 f4	a = .001 f5
1	15625	0.93280	0.06720	0.79468	0.87406	1.56866	1.04771	0.96088	0.88101	0.87475
2	62500	0.80130	0.19871	0.91573	0.66847	1.28060	0.82150	0.74498	0.67459	0.66908
3	140625	0.64004	0.35996	0.94542	0.47063	0.91558	0.58187	0.52625	0.47508	0.47108
4	250000	0.52830	0.47170	0.95564	0.35898	0.70203	0.44474	0.40186	0.36241	0.35932
5	390625	0.43512	0.56489	0.94266	0.27805	0.54015	0.34358	0.31081	0.28067	0.27831
6	562500	0.37372	0.62628	0.92755	0.22980	0.44295	0.28309	0.25645	0.23193	0.23002

Table A.2.b. Non-forested 2

$$f = (d * (1 + (a * \text{SqP}))) / (1 + Q)$$

etm+										
	n	d	Q	SqP	a = 0 f0	a = 1 f1	a = 0.25 f2	a = .125 f3	a = 0.01 f4	a = .001 f5
1	289	0.97924	0.02083	0.26858	0.95925	1.21689	1.02366	0.99146	0.96183	0.95951
2	1089	0.97062	0.02941	0.40346	0.94288	1.32330	1.03799	0.99043	0.94669	0.94326
3	2500	0.92520	0.07483	0.53079	0.86079	1.31769	0.97501	0.91790	0.86536	0.86124
4	4489	0.84161	0.15842	0.66320	0.72652	1.20834	0.84697	0.78675	0.73134	0.72700
5	6889	0.74917	0.25087	0.75481	0.59891	1.05098	0.71193	0.65542	0.60344	0.59937
6	10000	0.65970	0.34033	0.80475	0.49219	0.88828	0.59121	0.54170	0.49615	0.49259

ikonos										
	n	d	Q	SqP	a = 0 f0	a = 1 f1	a = 0.25 f2	a = .125 f3	a = 0.01 f4	a = .001 f5
1	15625	0.99046	0.00954	0.43963	0.98111	1.41243	1.08894	1.03502	0.98542	0.98154
2	62500	0.97330	0.02670	0.76170	0.94798	1.67006	1.12850	1.03824	0.95520	0.94870
3	140625	0.96084	0.03916	0.87219	0.92463	1.73108	1.12624	1.02544	0.93269	0.92544
4	250000	0.88537	0.11463	0.92376	0.79432	1.52808	0.97776	0.88604	0.80166	0.79505
5	390625	0.77346	0.22655	0.93290	0.63060	1.21888	0.77767	0.70413	0.63648	0.63118
6	562500	0.65304	0.34696	0.92601	0.48482	0.93377	0.59706	0.54094	0.48931	0.48527

Table A.3.a. Intermediate 1

$$f = (d * (1 + (a * \text{SqP}))) / (1 + Q)$$

etm+							a = 0	a = 1	a = 0.25	a = .125	a = 0.01	a = .001
	n	d	Q	SqP	f0	f1	f2	f3	f4	f5		
1	289	0.76817	0.23264	0.63659	0.62319	1.01991	0.72237	0.67278	0.62716	0.62358		
2	1089	0.66208	0.33824	0.75700	0.49474	0.86925	0.58837	0.54155	0.49848	0.49511		
3	2500	0.50360	0.49660	0.80923	0.33650	0.60880	0.40457	0.37053	0.33922	0.33677		
4	4489	0.39497	0.60517	0.84744	0.24606	0.45458	0.29819	0.27212	0.24814	0.24627		
5	6889	0.34925	0.65084	0.86394	0.21156	0.39433	0.25725	0.23441	0.21339	0.21174		
6	10000	0.35260	0.64747	0.87719	0.21403	0.40177	0.26096	0.23749	0.21590	0.21421		

ikonos							a = 0	a = 1	a = 0.25	a = .125	a = 0.01	a = .001
		d	Q	SqP	f0	f1	f2	f3	f4	f5		
1	15750	0.40502	0.59502	0.90975	0.25393	0.48493	0.31168	0.28280	0.25624	0.25416		
2	62500	0.44094	0.55907	0.93892	0.28283	0.54838	0.34921	0.31602	0.28548	0.28309		
3	140250	0.33895	0.66105	0.95755	0.20406	0.39945	0.25291	0.22848	0.20601	0.20425		
4	250000	0.28427	0.71574	0.96686	0.16568	0.32588	0.20573	0.18571	0.16728	0.16584		
5	391250	0.26073	0.73928	0.96101	0.14990	0.29397	0.18592	0.16791	0.15135	0.15005		
6	562500	0.26325	0.73675	0.95302	0.15158	0.29604	0.18769	0.16964	0.15302	0.15172		

Table A.3.b. Intermediate 2

$$f = (d * (1 + (a * \text{SqP}))) / (1 + Q)$$

etm+							a = 0	a = 1	a = 0.25	a = .125	a = 0.01	a = .001
	n	d	Q	SqP	f0	f1	f2	f3	f4	f5		
1	272	0.43382	0.56827	0.32108	0.27663	0.36544	0.29883	0.28773	0.27751	0.27672		
2	1122	0.39483	0.60571	0.56603	0.24589	0.38507	0.28069	0.26329	0.24728	0.24603		
3	2500	0.36560	0.63465	0.65645	0.22366	0.37047	0.26036	0.24201	0.22512	0.22380		
4	4422	0.34713	0.65302	0.75589	0.21000	0.36873	0.24968	0.22984	0.21158	0.21015		
5	6972	0.36446	0.63563	0.80833	0.22282	0.40294	0.26785	0.24534	0.22462	0.22300		
6	10000	0.35760	0.64246	0.83639	0.21772	0.39982	0.26325	0.24048	0.21954	0.21790		

ikonos							a = 0	a = 1	a = 0.25	a = .125	a = 0.01	a = .001
	n	d	Q	SqP	f0	f1	f2	f3	f4	f5		
1	15625	0.38099	0.61905	0.86923	0.23532	0.43986	0.28645	0.26089	0.23736	0.23552		
2	62500	0.34173	0.65828	0.91851	0.20607	0.39535	0.25339	0.22973	0.20797	0.20626		
3	140625	0.31937	0.68064	0.93891	0.19003	0.36845	0.23463	0.21233	0.19181	0.19021		
4	250000	0.29954	0.70046	0.95142	0.17615	0.34375	0.21805	0.19710	0.17783	0.17632		
5	390625	0.30728	0.69273	0.95771	0.18153	0.35538	0.22499	0.20326	0.18327	0.18170		
6	562500	0.30922	0.69078	0.94909	0.18288	0.35646	0.22628	0.20458	0.18462	0.18306		

APPENDIX B

Summaries for Increasing Support of Fragmentation Study






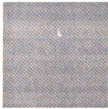
 <p>17 x 17 cells $f = 0, \alpha = 0$ $f = 0, \alpha = 0.001$ $\gamma = 0$ $\text{var} = 0$ $\text{gam1/var} = 0$ $\text{Moran's I} = \text{NaN}$ $\text{Min} = \text{NaN}$ $\text{Max} = \text{NaN}$ $\text{Geary's C} = \text{NaN}$ $\text{Min} = \text{NaN}$ $\text{Max} = \text{NaN}$</p>	 <p>33 x 33 cells $f = 0, \alpha = 0$ $f = 0, \alpha = 0.001$ $\gamma = 0$ $\text{var} = 0$ $\text{gam1/var} = 0$ $\text{Moran's I} = \text{NaN}$ $\text{Min} = \text{NaN}$ $\text{Max} = \text{NaN}$ $\text{Geary's C} = \text{NaN}$ $\text{Min} = \text{NaN}$ $\text{Max} = \text{NaN}$</p>	 <p>50 x 50 cells $f = 0.003008427, \alpha = 0$ $f = 0.003009, \alpha = 0.001$ $\gamma = 0.003618$ $\text{var} = 0.005964$ $\text{gam1/var} = 0.606595$ $\text{Moran's I} = 0.564^*$ $\text{Min} = -0.00639$ $\text{Max} = 0.04437$ $\text{Geary's C} = 0.44^*$ $\text{Min} = 0.955$ $\text{Max} = 1.027$</p>
 <p>67 x 67 cells $f = 0.00167361, \alpha = 0$ $f = 0.001674, \alpha = 0.001$ $\gamma = 0.001244$ $\text{var} = 0.00333$ $\text{gam1/var} = 0.37347$ $\text{Moran's I} = 0.5652^*$ $\text{Min} = -0.00349$ $\text{Max} = 0.04681$ $\text{Geary's C} = 0.4347^*$ $\text{Min} = 0.949$ $\text{Max} = 1.024$</p>	 <p>83 x 83 cells $f = 0.001089608, \alpha = 0$ $f = 0.00109, \alpha = 0.001$ $\gamma = 0.000961$ $\text{var} = 0.002173$ $\text{gam1/var} = 0.442239$ $\text{Moran's I} = 0.5657^*$ $\text{Min} = -0.00227$ $\text{Max} = 0.03130$ $\text{Geary's C} = 0.4342^*$ $\text{Min} = 0.960$ $\text{Max} = 1.023$</p>	 <p>100 x 100 cells $f = 0.000750525, \alpha = 0$ $f = 0.000751, \alpha = 0.001$ $\gamma = 0.00066$ $\text{var} = 0.001498$ $\text{gam1/var} = 0.440571$ $\text{Moran's I} = 0.566^*$ $\text{Min} = -0.00156$ $\text{Max} = 0.03191$ $\text{Geary's C} = 0.4339^*$ $\text{Min} = 0.968$ $\text{Max} = 1.022$</p>

Figure B.1.a. Summaries of increasing support for fragmentation study: forested 1



Figure B.1.b. Summaries of increasing support for fragmentation study: forested 2

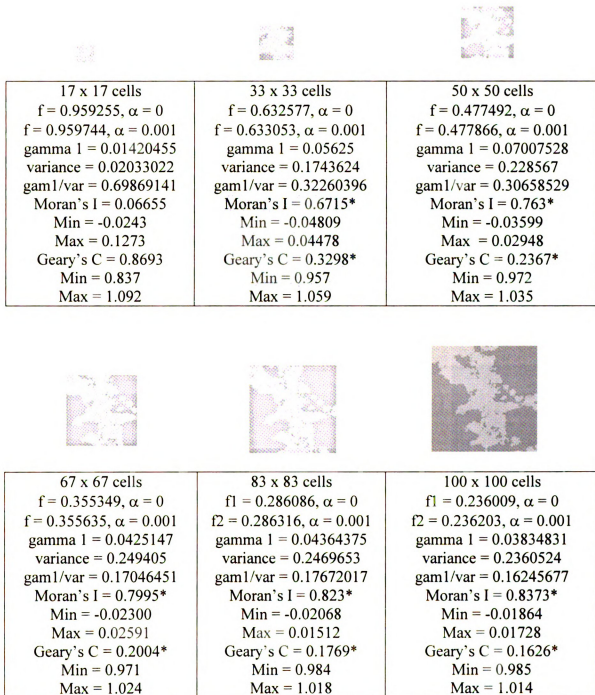


Figure B.2.a. Summaries of increasing support for fragmentation study: non-forested 1

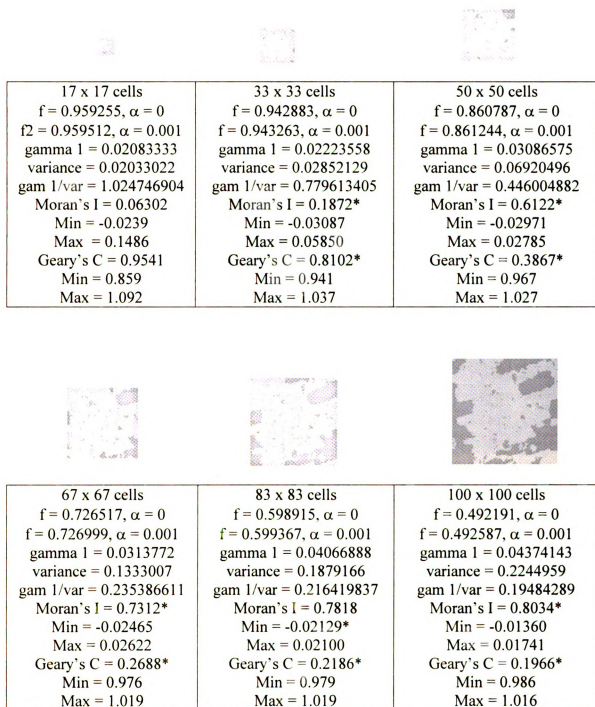


Figure B.2.b. Summaries of increasing support for fragmentation study: non-forested 2







 <p>17 x 17 cells $f = 0.623188, \alpha = 0$ $f = 0.627155, \alpha = 0.001$ $\text{gamma } l = 0.10795455$ $\text{variance} = 0.1780869$ $\text{gam } l/\text{var} = 0.606190292$ $\text{Moran's } I = 0.3893^*$ $\text{Min} = -0.08526$ $\text{Max} = 0.09070$ $\text{Geary's } C = 0.6099^*$ $\text{Min} = 0.887$ $\text{Max} = 1.073$</p>	 <p>33 x 33 cells $f = 0.494737, \alpha = 0$ $f = 0.495112, \alpha = 0.001$ $\text{gamma } l = 0.10336538$ $\text{variance} = 0.2237316$ $\text{gam } l/\text{var} = 0.462006172$ $\text{Moran's } I = 0.5405^*$ $\text{Min} = -0.04096$ $\text{Max} = 0.04882$ $\text{Geary's } C = 0.459^*$ $\text{Min} = 0.952$ $\text{Max} = 1.051$</p>	 <p>50 x 50 cells $f = 0.336496, \alpha = 0$ $f = 0.336769, \alpha = 0.001$ $\text{gamma } l = 0.10002091$ $\text{variance} = 0.249987$ $\text{gam } l/\text{var} = 0.400104445$ $\text{Moran's } I = 0.6775^*$ $\text{Min} = -0.02945$ $\text{Max} = 0.03546$ $\text{Geary's } C = 0.3224^*$ $\text{Min} = 0.971$ $\text{Max} = 1.031$</p>
 <p>67 x 67 cells $f = 0.246058, \alpha = 0$ $f = 0.246267, \alpha = 0.001$ $\text{gamma } l = 0.05857078$ $\text{variance} = 0.2389677$ $\text{gam } l/\text{var} = 0.245099149$ $\text{Moran's } I = 0.7164^*$ $\text{Min} = -0.02965$ $\text{Max} = 0.02164$ $\text{Geary's } C = 0.2836^*$ $\text{Min} = 0.976$ $\text{Max} = 1.024$</p>	 <p>83 x 83 cells $f = 0.21156, \alpha = 0$ $f = 0.211743, \alpha = 0.001$ $\text{gamma } l = 0.056966$ $\text{variance} = 0.2272752$ $\text{gam } l/\text{var} = 0.250647673$ $\text{Moran's } I = 0.7487^*$ $\text{Min} = -0.02459$ $\text{Max} = 0.01865$ $\text{Geary's } C = 0.2511^*$ $\text{Min} = 0.980$ $\text{Max} = 1.019$</p>	 <p>100 x 100 cells $f = 0.214026, \alpha = 0$ $f = 0.214214, \alpha = 0.001$ $\text{gamma } l = 0.05148216$ $\text{variance} = 0.2282732$ $\text{gam } l/\text{var} = 0.225528709$ $\text{Moran's } I = 0.7736^*$ $\text{Min} = -0.01605$ $\text{Max} = 0.01472$ $\text{Geary's } C = 0.2263^*$ $\text{Min} = 0.984$ $\text{Max} = 1.015$</p>

Figure B.3.a. Summaries of increasing support for fragmentation study: intermediate 1

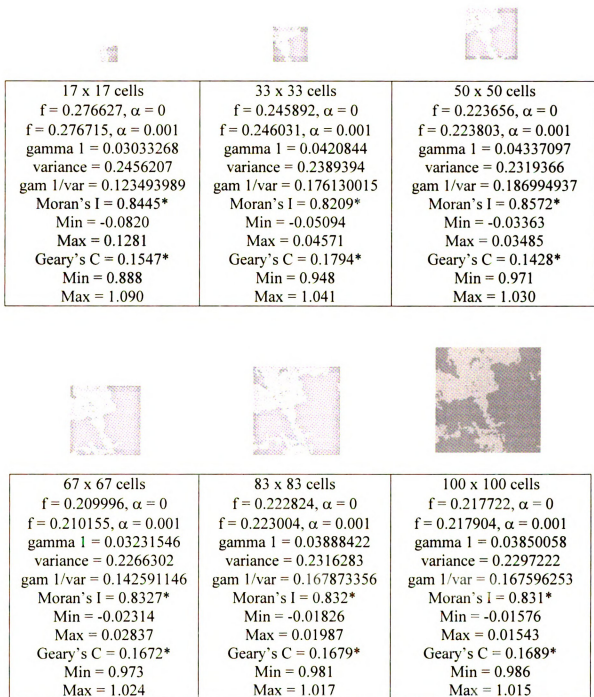


Figure B.3.b. Summaries of increasing support for fragmentation study: intermediate 2

APPENDIX C

Variograms for Increasing Supports of Two Cases Each of Three Forest Scenarios

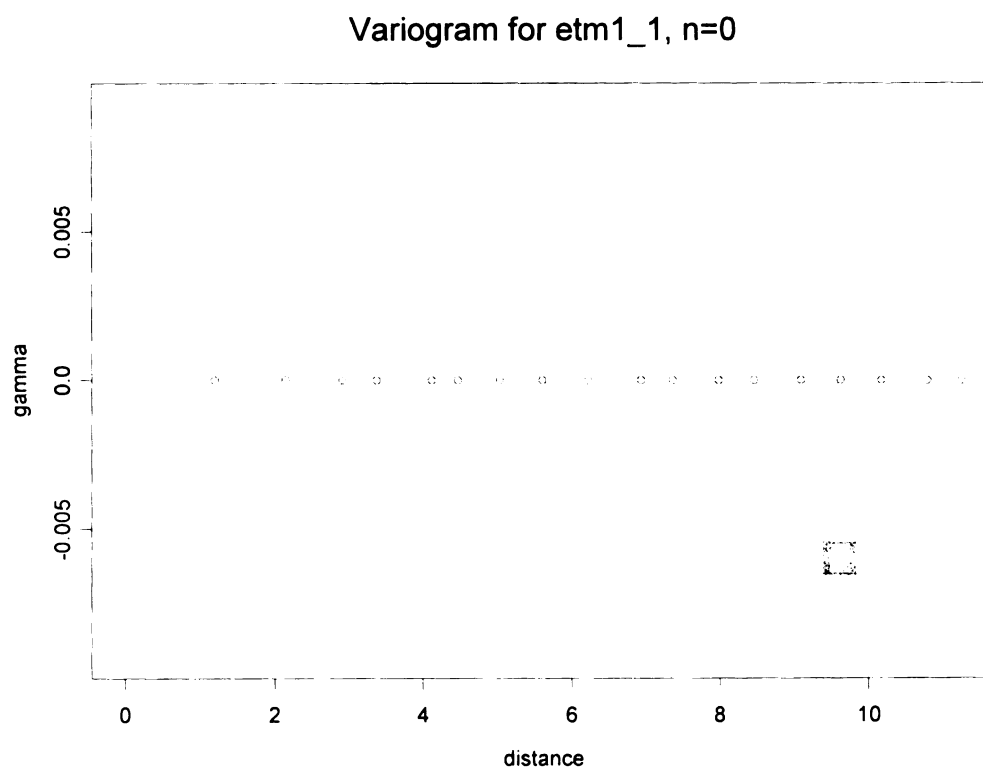


Figure C.1.1.a. Forested 1, 17 x 17 cells

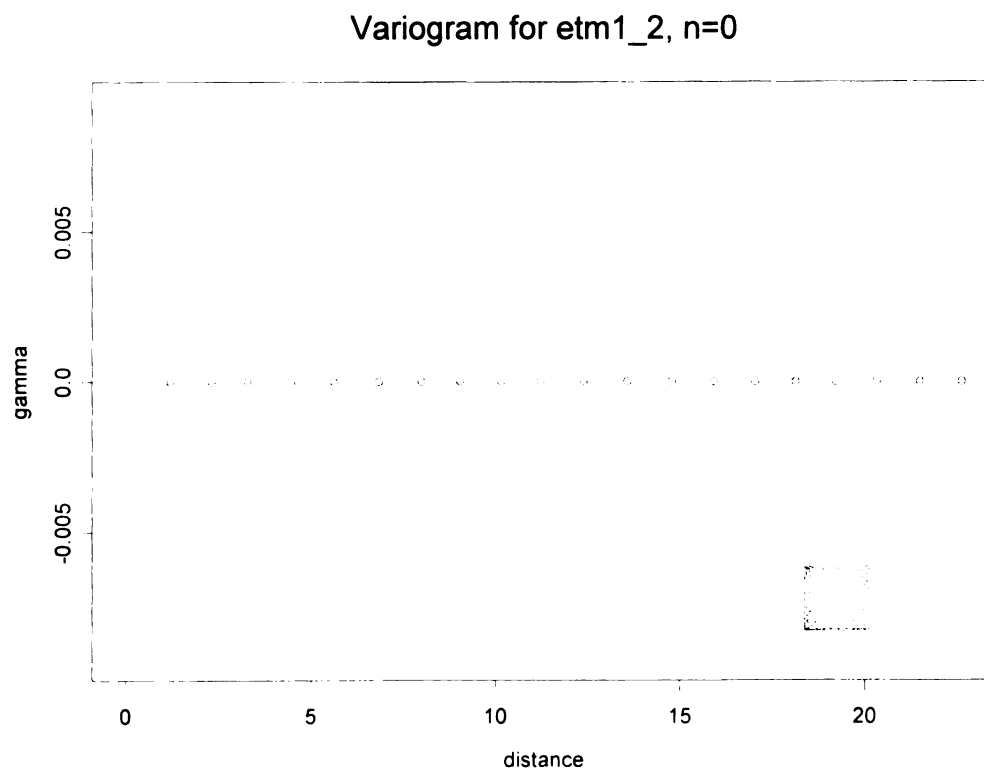


Figure C.1.1.b. Forested 1, 33 x 33 cells

Variogram for etm1_3, $r=1.95$, $s=0.0065$, $n=0$

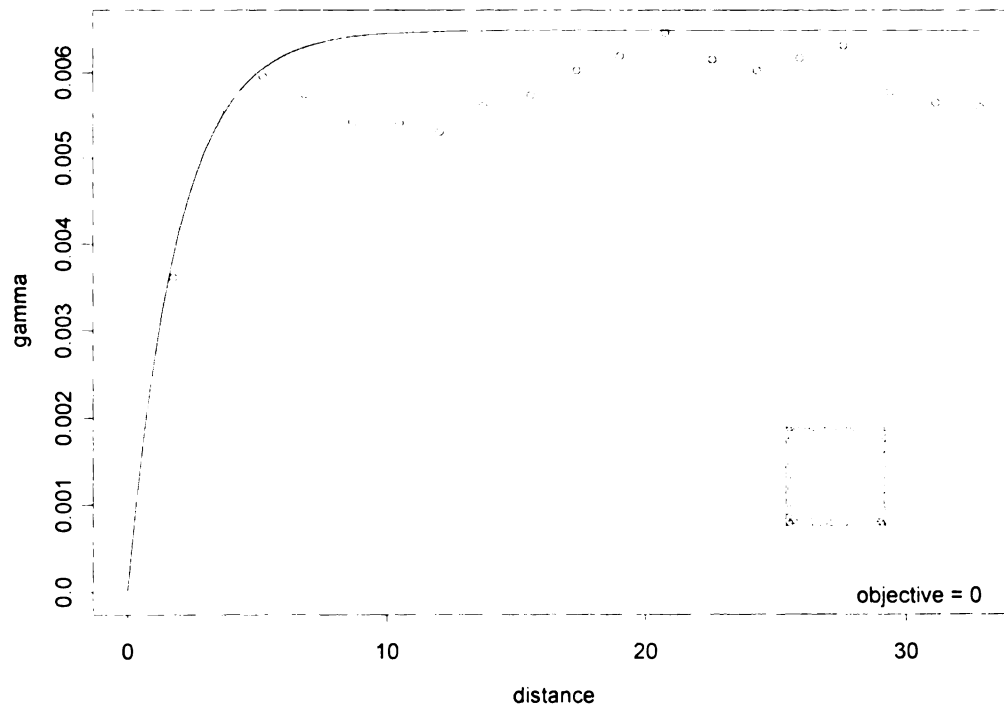


Figure C.1.1.c. Forested 1, 50 x 50 cells

Variogram for etm1_4, $r=3$, $s=0.00395$, $n=.0003$

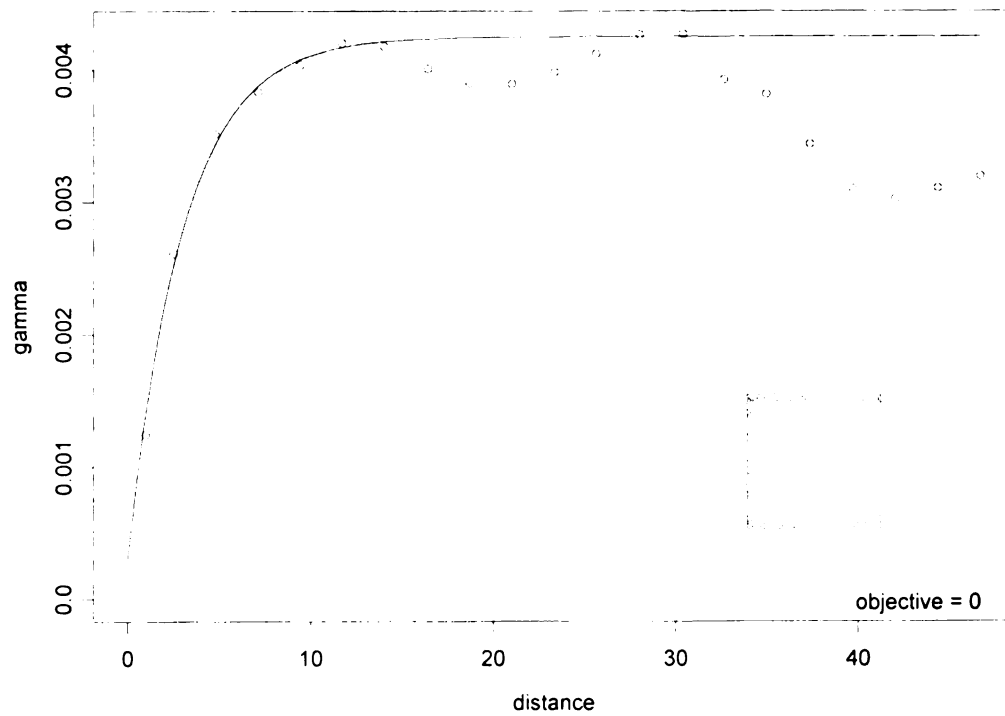


Figure C.1.1.d. Forested 1, 67 x 67 cells

Variogram for etm1_5, $r=2.5$, $s=0.00245$, $n=.00015$

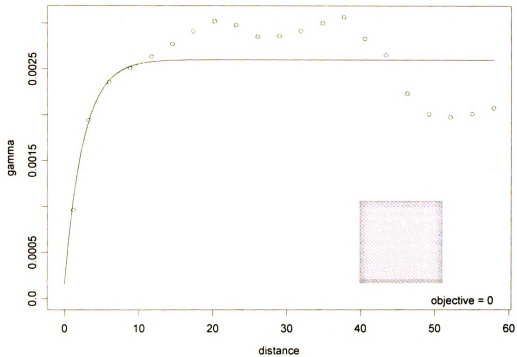


Figure C.1.1.e. Forested 1, 83 x 83 cells

Variogram for etm1_6, $r=2.5$, $s=0.00175$, $n=0$

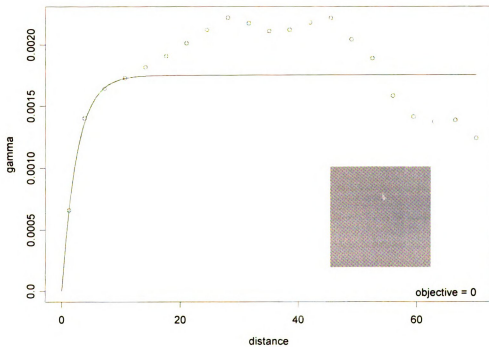


Figure C.1.1.f. Forested 1, 100 x 100 cells

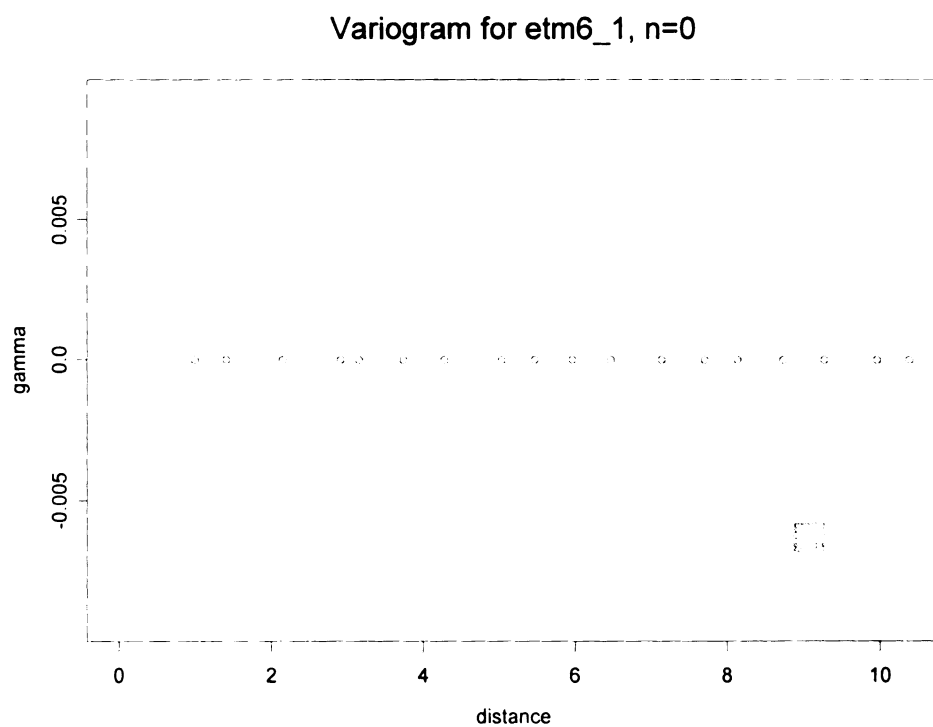


Figure C.1.2.a. Forested 2, 17 x 17 cells

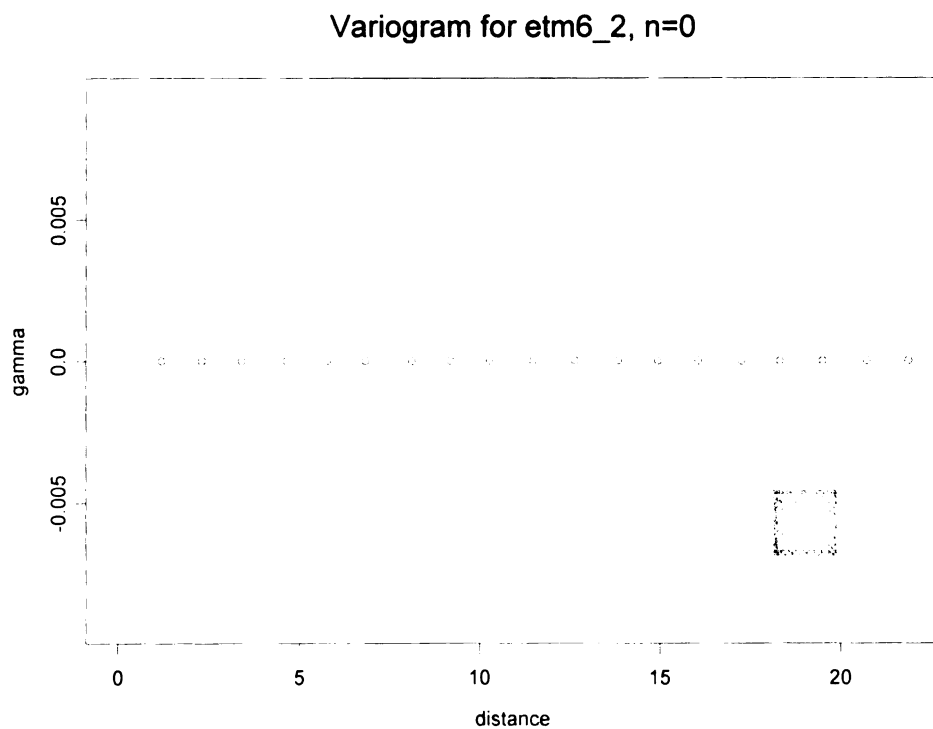


Figure C.1.2.b. Forested 2, 33 x 33 cells

Variogram for etm6_3, $r=1.5$, $s=.0063$, $n=.001$

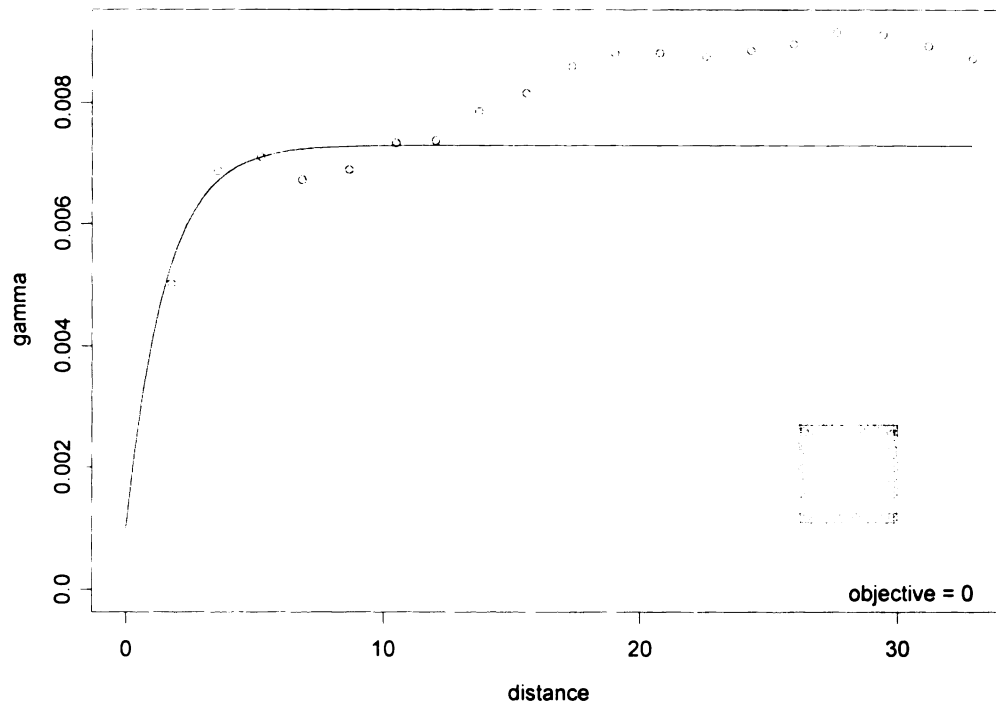


Figure C.1.2.c. Forested 2, 50 x 50 cells

Variogram for etm6_4, $r=1.75$, $s=.015$, $n=0$

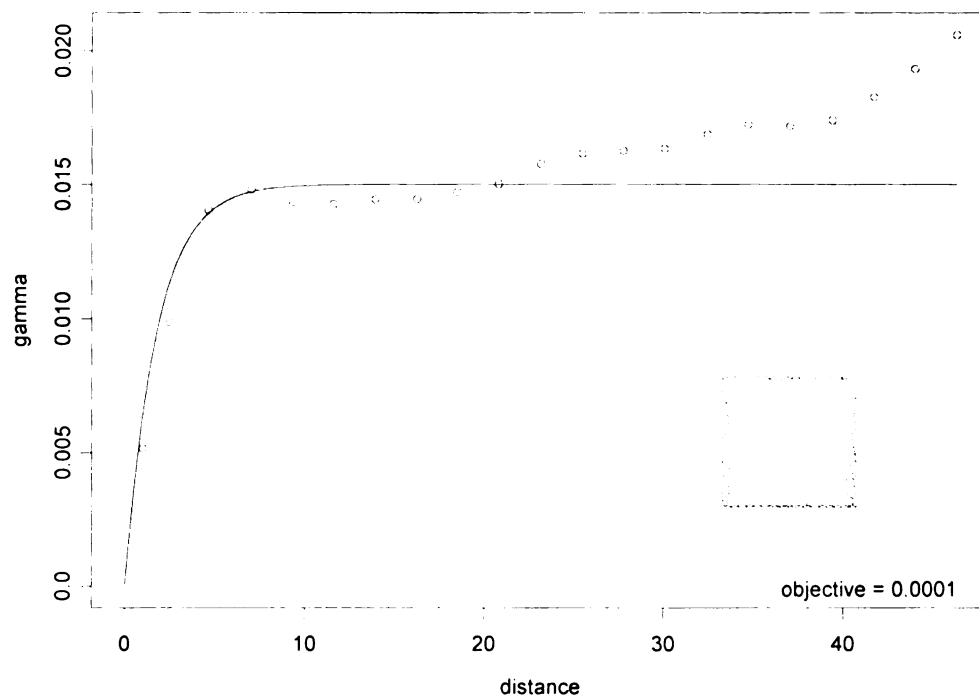


Figure C.1.2.d. Forested 2, 63 x 63 cells

Variogram for etm6_5, $r=8$, $s=.0675$, $n=.01$

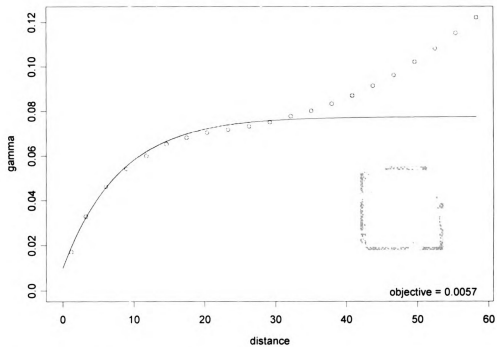


Figure C.1.2.e. Forested 2, 83 x 83 cells

Variogram for etm6_6, $r=14$, $s=.16$, $n=.01$

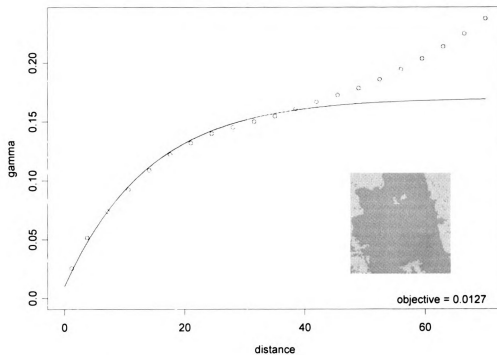


Figure C.1.2.f. Forested 2, 100 x 100 cells

Variogram for etm2_1, $r=1.6$, $s=0.0063$, $n=0.011$

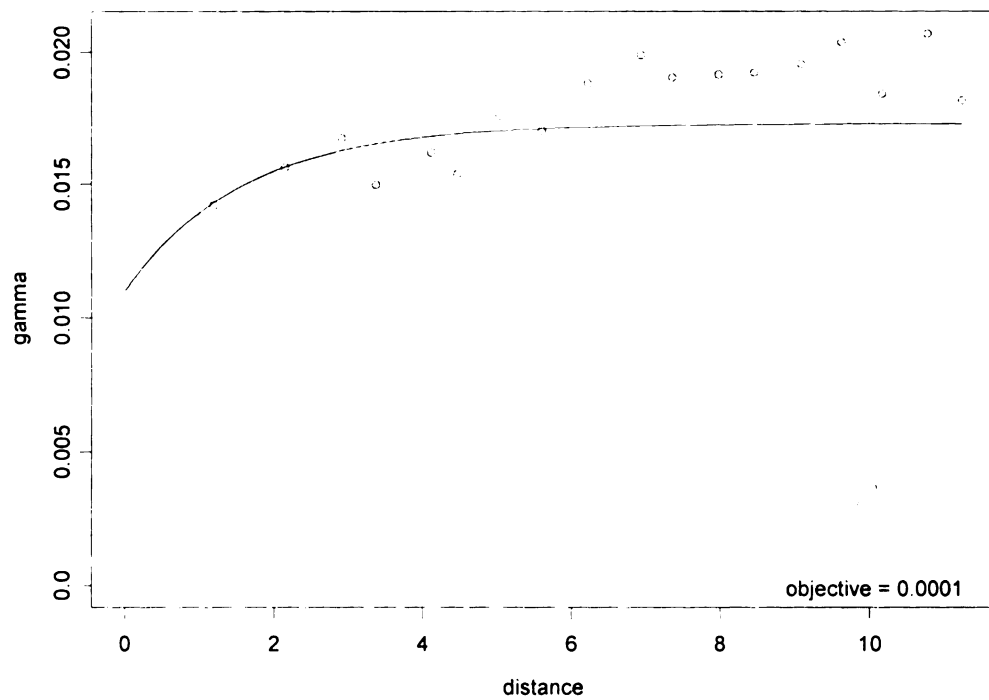


Figure C.2.1.a. Non-forested 1, 17 x 17 cells

Variogram for etm2_2, $r=1.8$, $s=0.1$, $n=0.01$

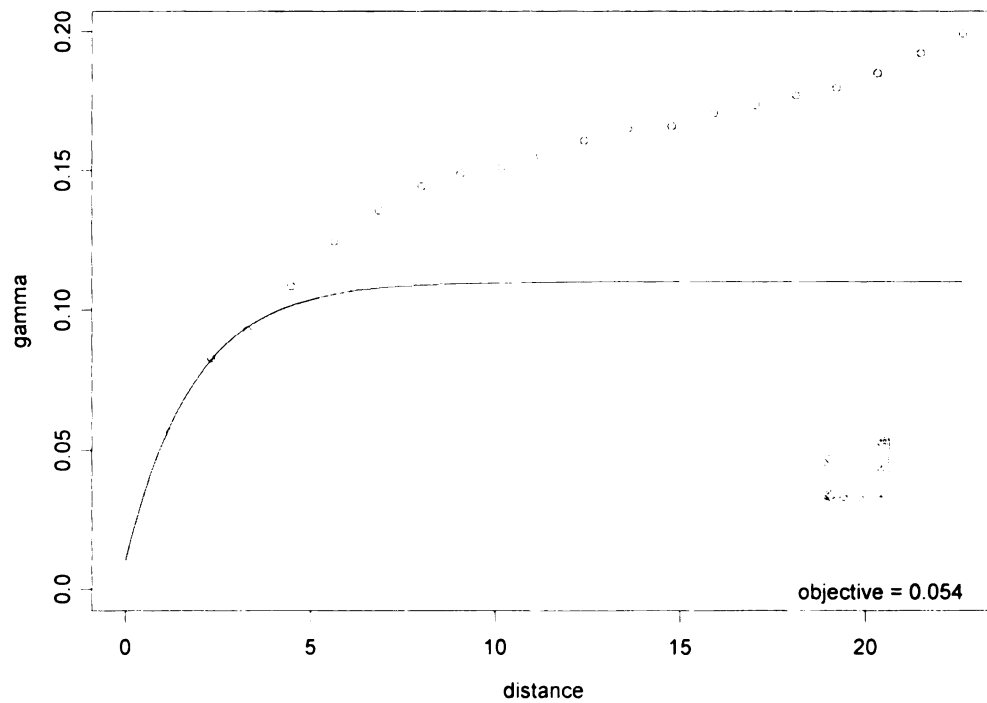


Figure C.2.1.b. Non-forested 1, 33 x 33 cells

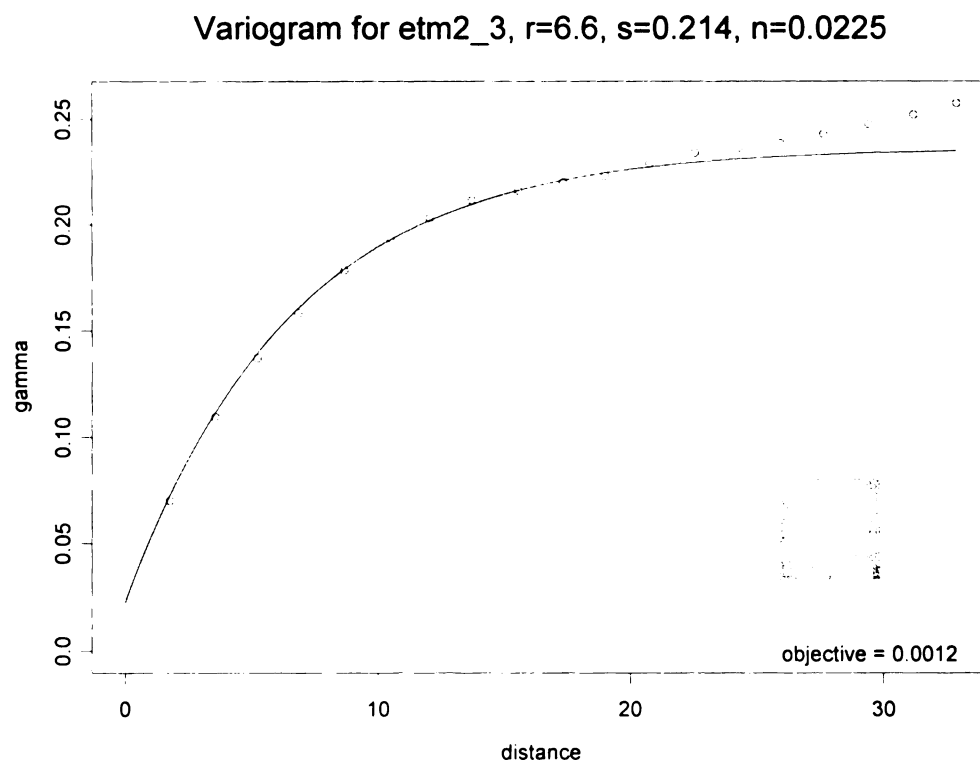


Figure C.2.1.c. Non-forested 1, 50 x 50 cells

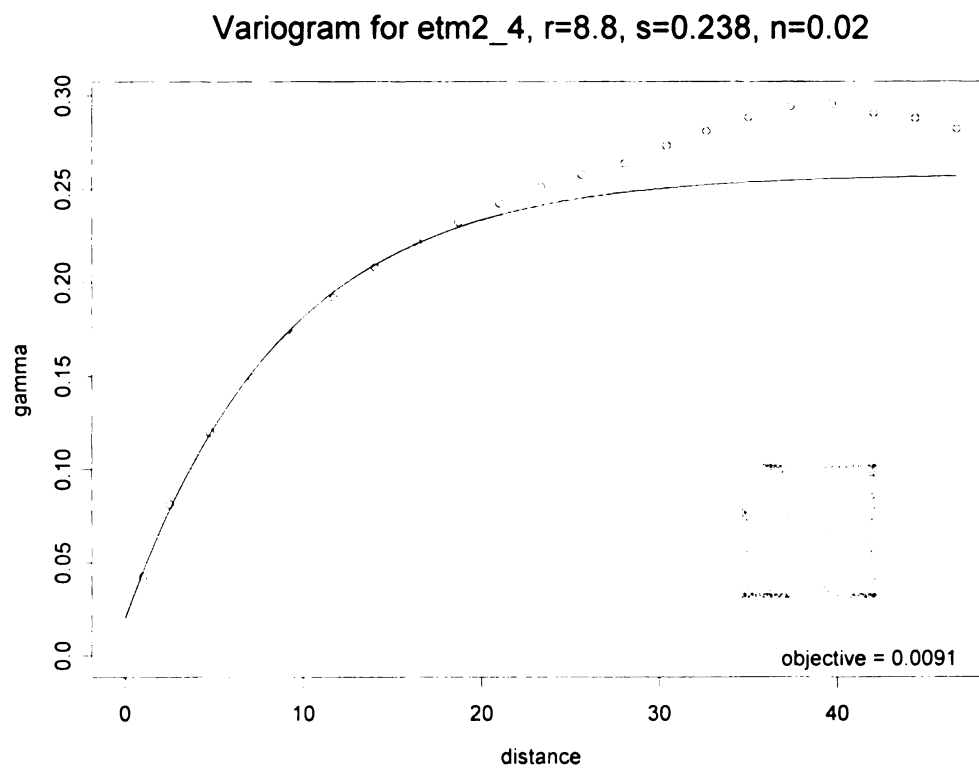


Figure C.2.1.d. Non-forested 1, 67 x 67 cells

Variogram for etm2_5, $r=10.5$, $s=0.226$, $n=0.02$

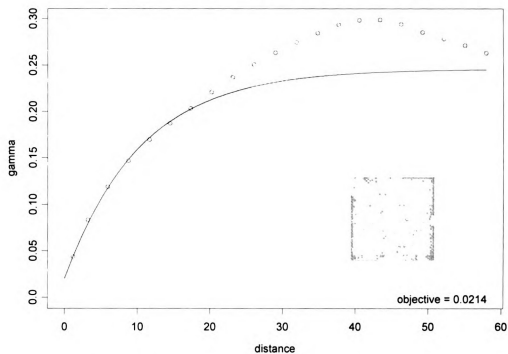


Figure C.2.1.e. Non-forested 1, 83 x 83 cells

Variogram for etm2_6, $r=7.7$, $s=0.178$, $n=0.015$

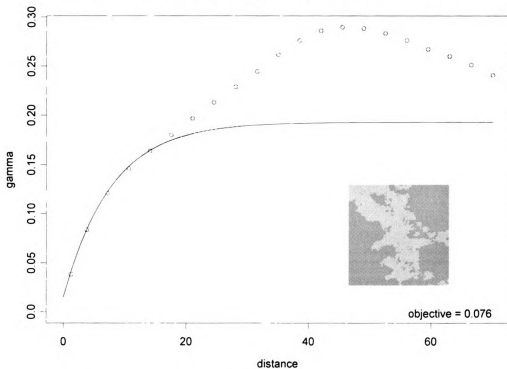


Figure C.2.1.f. Non-forested 1, 100 x 100 cells

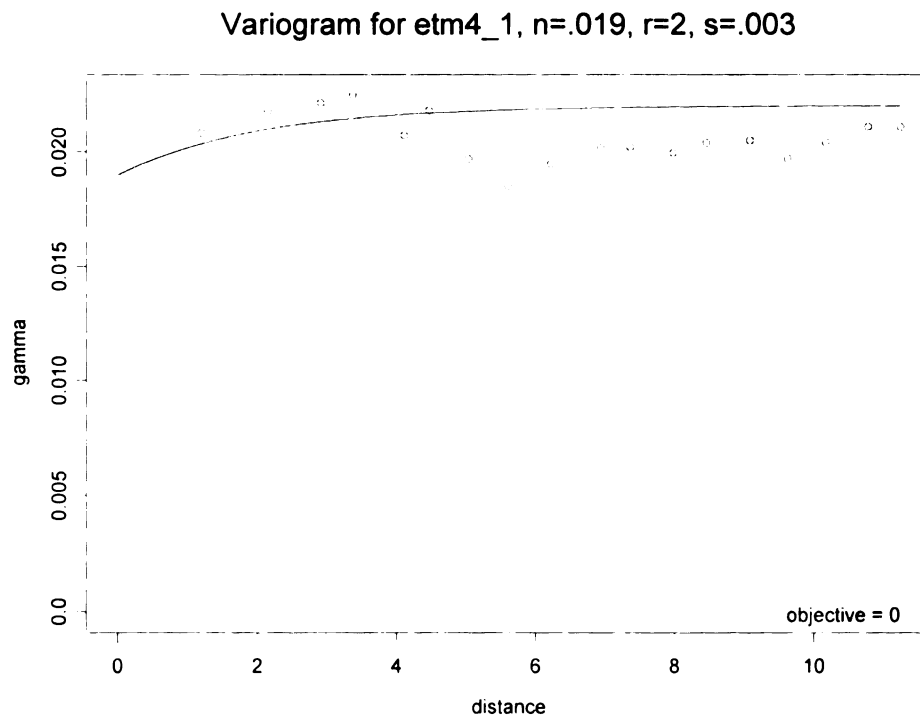


Figure C.2.2.a. Non-forested 2, 17 x 17 cells

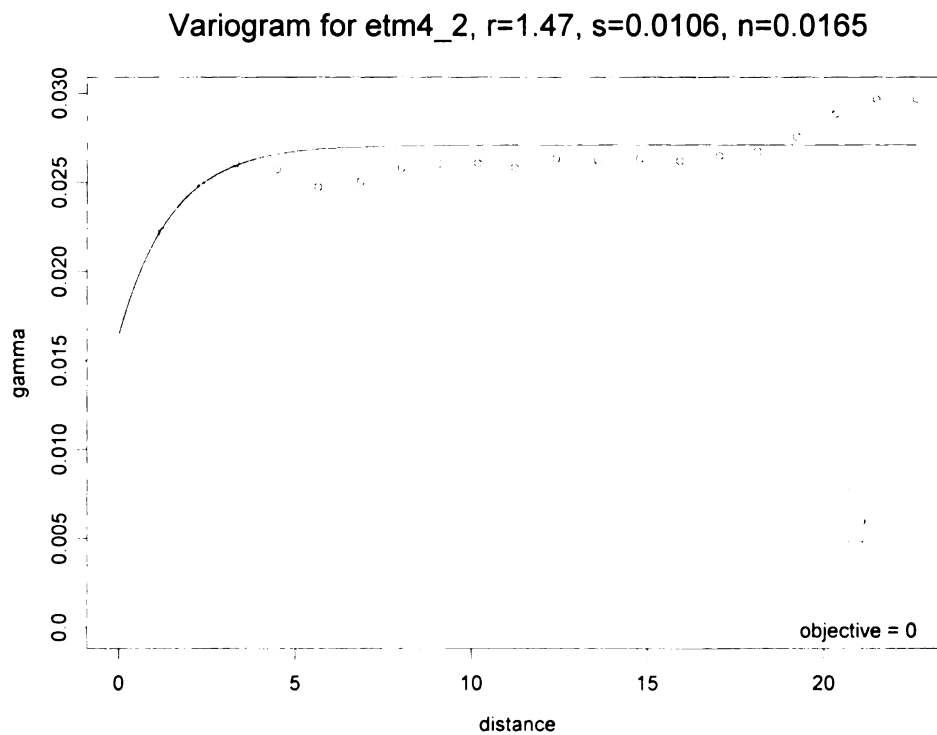


Figure C.2.2.b. Non-forested 2, 33 x 33 cells

Variogram for etm4_3, $n=.015$, $r=3.5$, $s=.041$

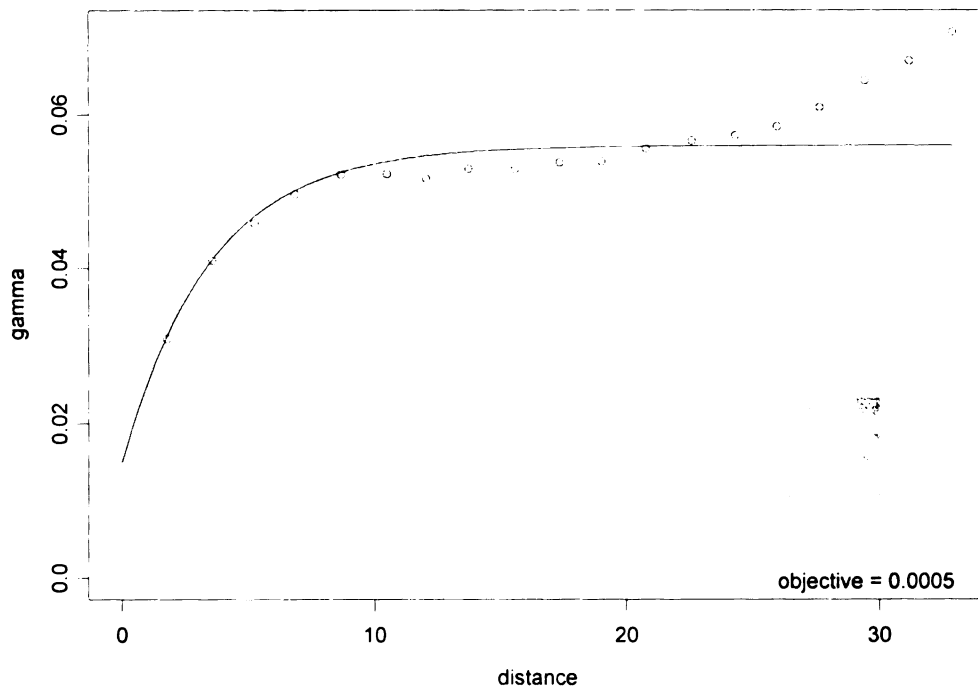


Figure C.2.2.c. Non-forested 2, 50 x 50 cells

Variogram for etm4_4, $r=4.2$, $s=0.0805$, $n=0.015$

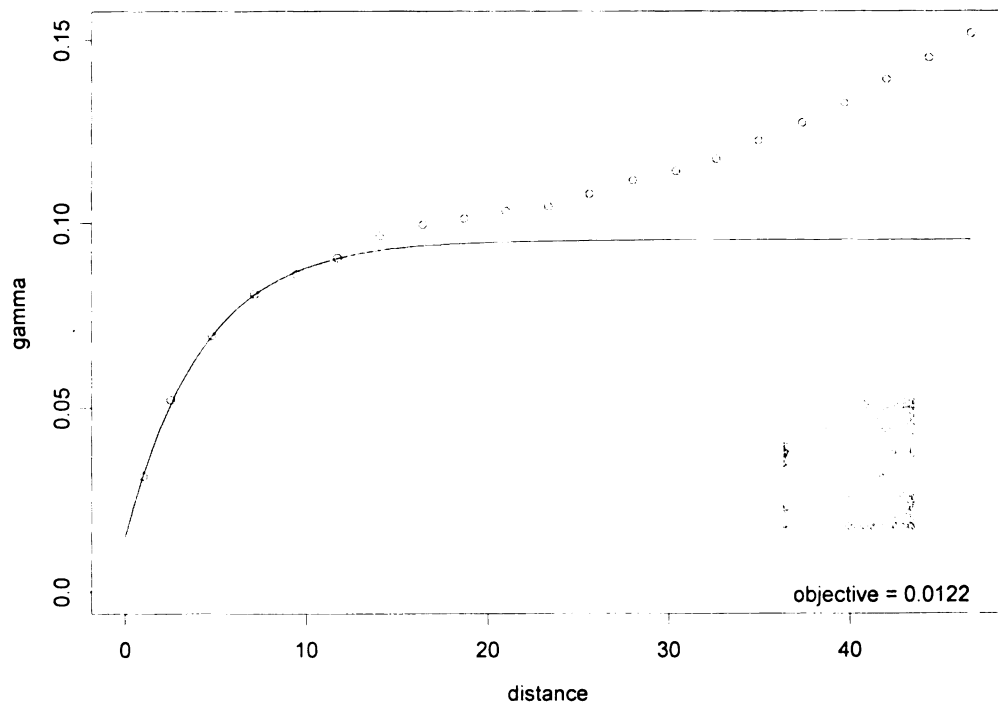


Figure C.2.2.d. Non-forested 2, 67 x 67 cells

Variogram for etm4_5, $r=6.1$, $s=0.137$, $n=0.017$

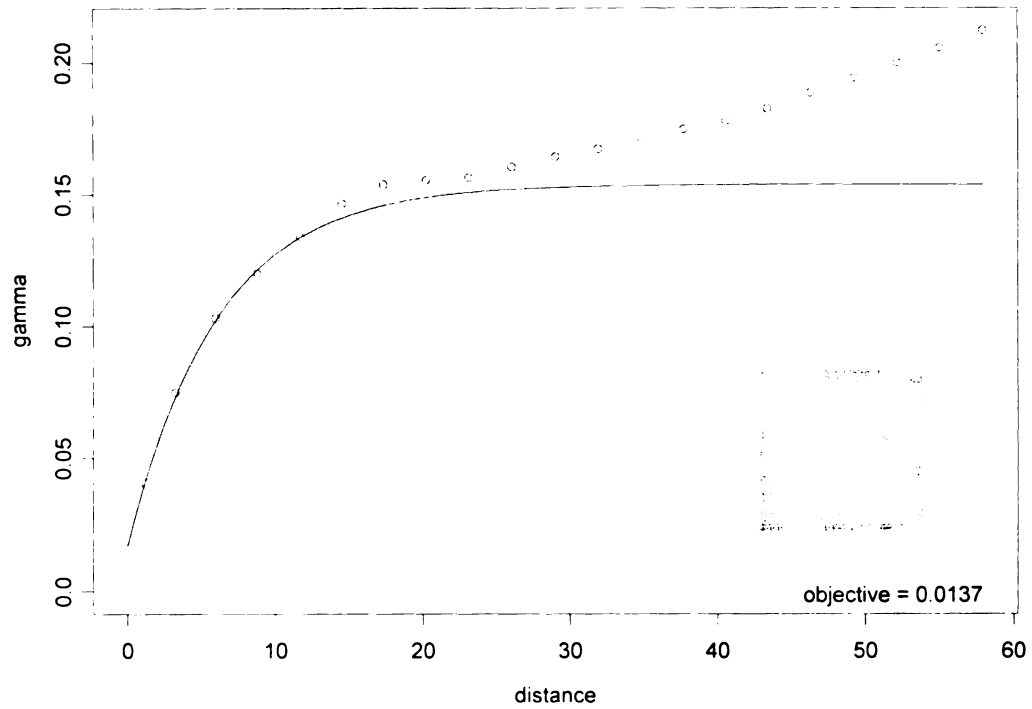


Figure C.2.2.e. Non-forested 2, 83 x 83 cells

Variogram for etm4_6, $r=8$, $s=0.19$, $n=0.02$

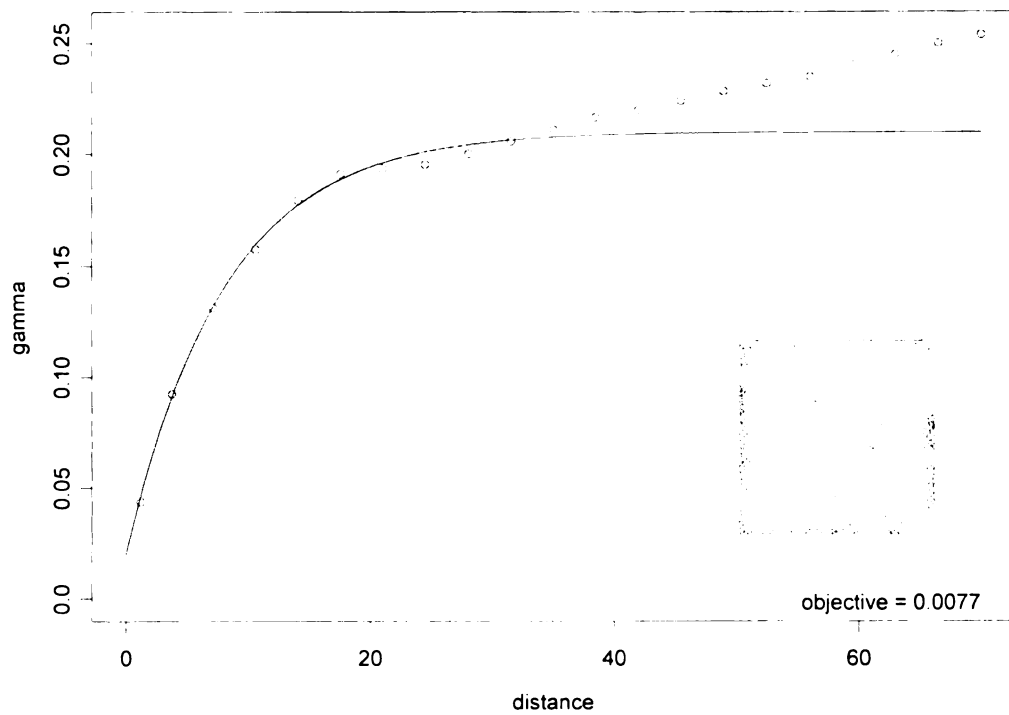


Figure C.2.2.f. Non-forested 2, 100 x 100 cells

Variogram for etm3_1, $n=.07$, $r=3.5$, $s=.135$

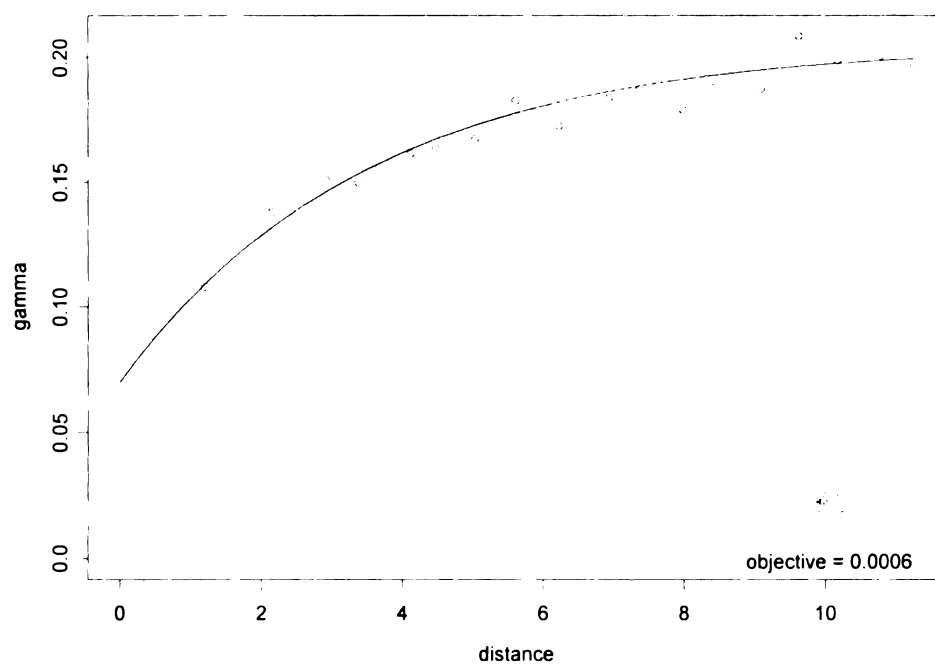


Figure C.3.1.a. Intermediate 1, 17 x 17 cells

Variogram for etm3_2, $r=1.5$, $s=0.173$, $n=0.01$

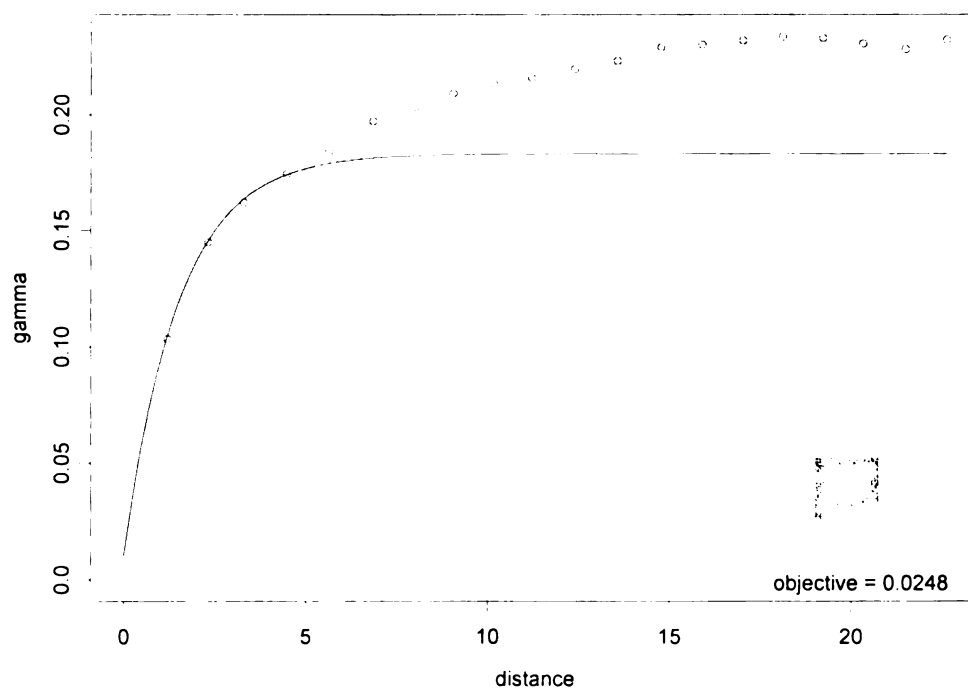


Figure C.3.1.b. Intermediate 1, 33 x 33 cells

Variogram for etm3_3, $r=4.5$, $s=0.176$, $n=0.045$

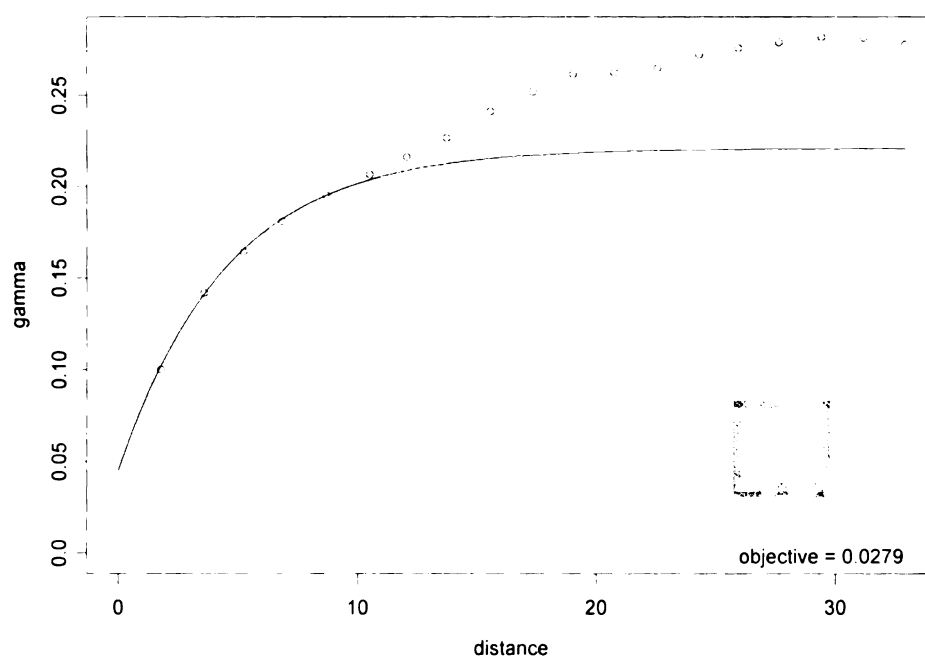


Figure C.3.1.c. Intermediate 1, 50 x 50 cells

Variogram for etm3_4, $r=4.4$, $s=0.176$, $n=0.025$

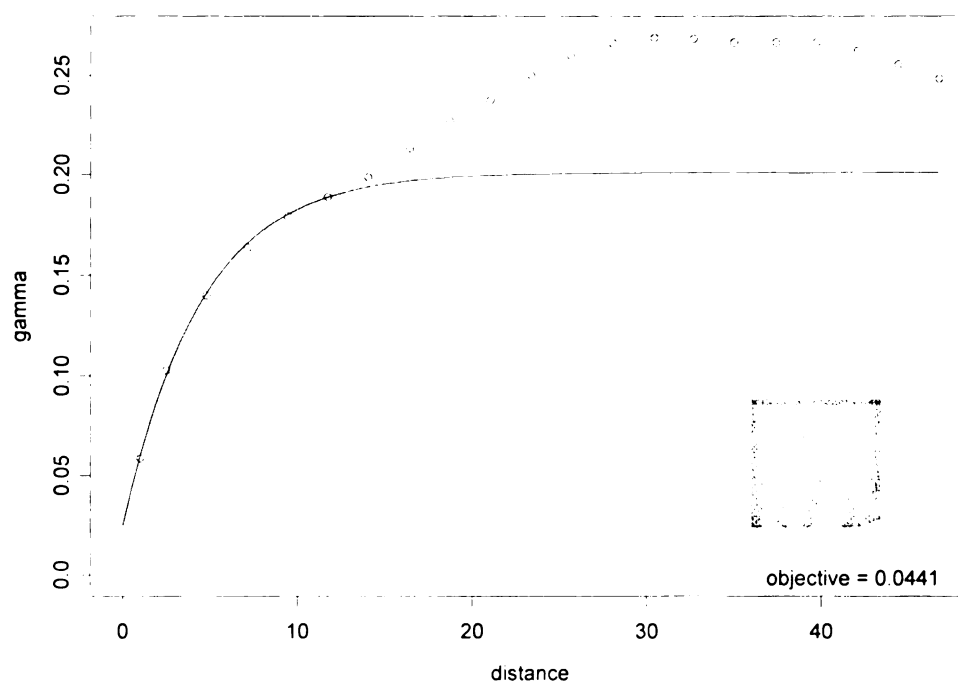


Figure C.3.1.d. Intermediate 1, 67 x 67 cells

Variogram for etm3_5, $r=5$, $s=0.152$, $n=0.025$

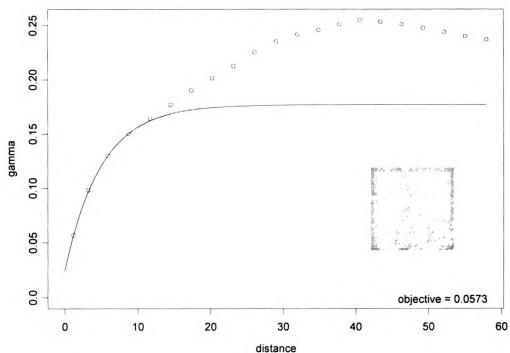


Figure C.3.1.e. Intermediate 1, 83 x 83

Variogram for etm3_6, $r=5.8$, $s=0.148$, $n=0.025$

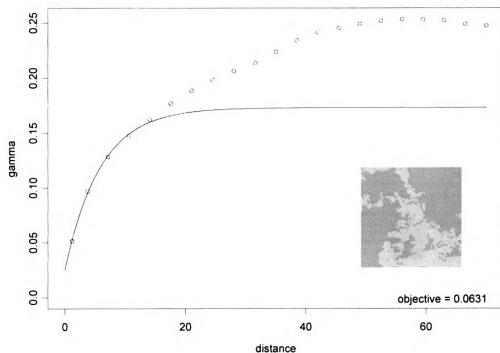


Figure C.3.1.f Intermediate 1, 100 x 100

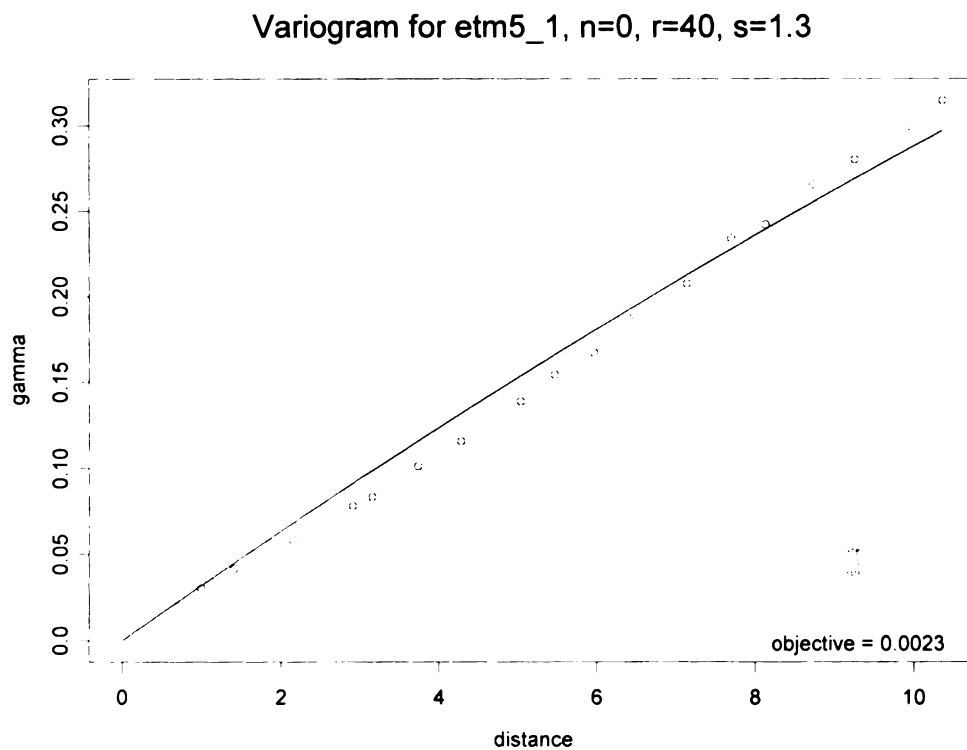


Figure C.3.2.a. Intermediate 2, 17 x 17 cells

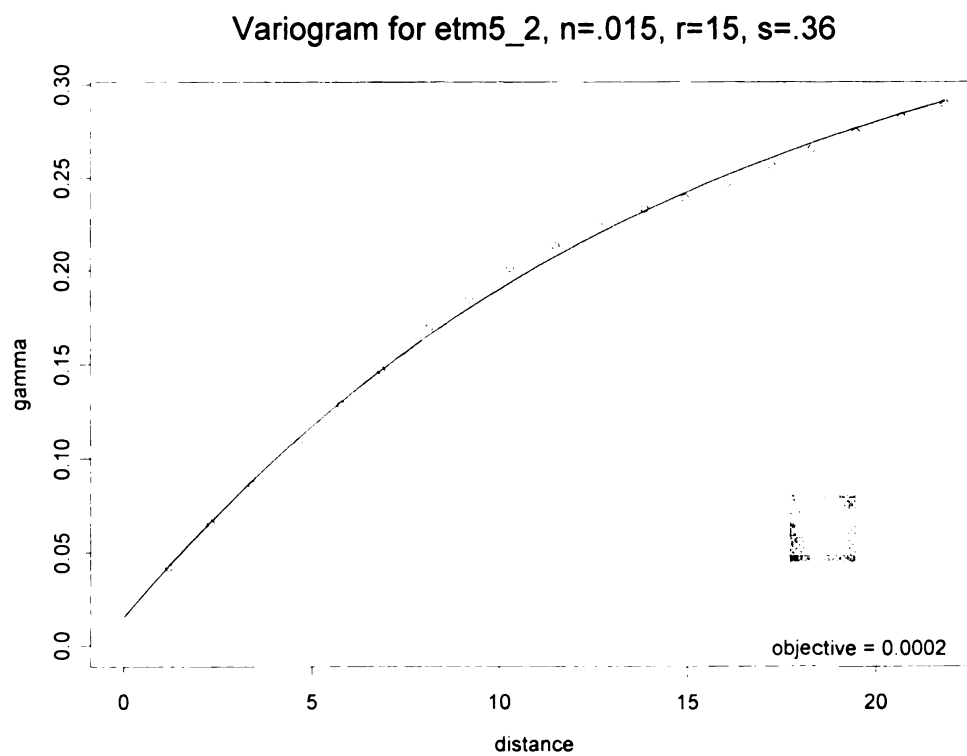


Figure C.3.2.b. Intermediate 2, 33 x 33 cells

Variogram for etm5_3, $r=15$, $s=0.265$, $n=0.015$

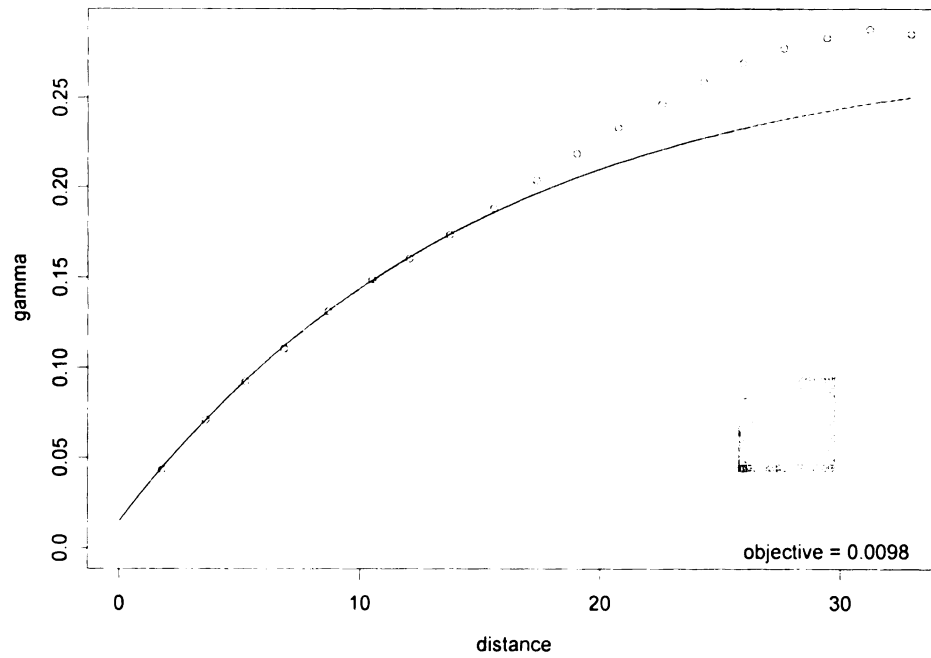


Figure C.3.2.c. Intermediate 2, 50 x 50 cells

Variogram for etm5_4, $r=6.7$, $s=0.138$, $n=0.015$

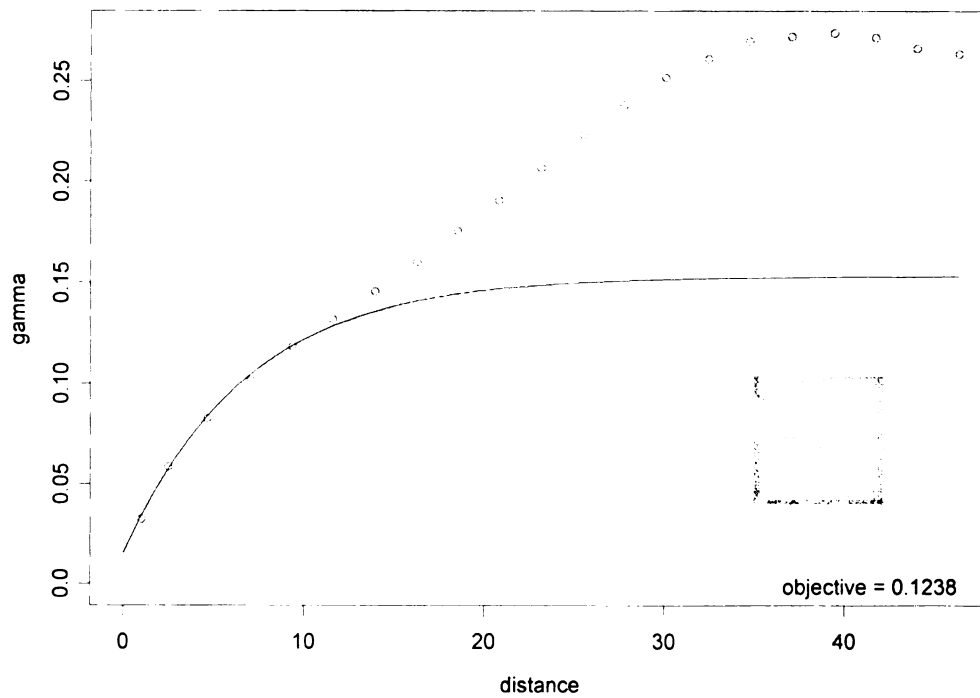


Figure C.3.2.d. Intermediate 2, 67 x 67

Variogram for etm5_5, $r=8.5$, $s=0.16$, $n=0.02$

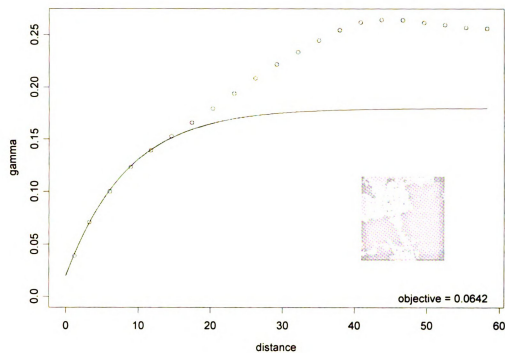


Figure C.3.2.e. Intermediate 2, 83 x 83 cells

Variogram for etm5_6, $r=10$, $s=0.17$, $n=0.02$

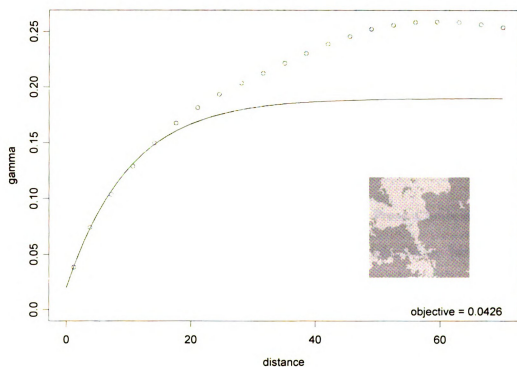


Figure C.3.2.f. Intermediate 2, 100 x 100 cells

LITERATURE CITED

- Atkinson, P.M. and N.J. Tate. 2000. Spatial Scale Problems and Geostatistical Solutions: A Review. *Professional Geographer*. **52**(4): 607-623.
- Arima, E., R. Walker, S. Perz, and M. Caldas. (unpub) Spatial process of logging roads extension in the Brazilian Amazon. Paper presented during the 2003 99th Annual Conference of the Association of American Geographers.
- Bailey, T.C. and A.C. Gatrell. 1995. Interactive Spatial Data Analysis. Prentice-Hill. New York.
- Bastian, Olaf. 2001. Landscape Ecology – towards a unified discipline? *Landscape Ecology*. **16**: 757-766.
- Cain, D.H., K. Riitters, and K. Orvis. 1997. A multi-scale analysis of landscape statistics. *Landscape Ecology*. **12**: 199-212.
- Cressie, N. 1993. Statistics for Spatial Data. rev ed. John Wiley & Sons. New York.
- de Cola, E. 1989. Fractal analysis of a classified landsat scene. *Photogrammetric Engineering and Remote Sensing*. **5**(5): 601-610.
- Dungan, J.L. 2001. Scaling Up and Scaling Down: The Relevance of the Support Effect on Remote Sensing of Vegetation. *In*. Modelling Scale in Geographic Information Science. Tate, N.J. and P.M. Atkinson, eds. John Wiley and Sons. Chichester, England.
- Eastman, J. R. 1996. IDRISI for Windows user's guide. Clark Labs for Cartographic Technology and Geographic Analysis, Clark University, Worcester, Massachusetts.
- ESRI. 1992. GRID Command Reference. Environmental Systems Research Institute, Inc. Redlands, CA.
- Forman, R.T.T. 1995. Land Mosaics. Cambridge University Press. Cambridge, UK.
- Forman, R.T.T. and M. Godron. 1986. Landscape Ecology. John Wiley. New York.
- Frohn, R. 1998. Remote Sensing for Landscape Ecology. Lewis Publishers. New York.
- Gergel, S.E. and M.G. Turner. (eds.) 2002. Learning Landscape Ecology: A Prctical Guide to Concepts and Techniques. Springer-Verlag. New York.
- Golley, F. 1989. Paradigm Shift: Editor's comment. *Landscape Ecology*. **3**(2): 65-66.

- Hay, G.J., D.J. Marceau, P. Dube, and A. Bouchard. 2001. A multiscale framework for landscape analysis: Object-specific analysis and upscaling. *Landscape Ecology*. **16**: 471-490.
- Hurd, J.D., E.H. Wilson, D.L. Civco. A Forest Fragmentation Index to Quantify the Rate of Forest Change.
URL:http://resac.uconn.edu/publications/presentations/hurd_asprs2002.ppt.
- Johnston, R.J. 1978. Multivariate statistical analysis in geography: A primer on the general linear model. Longman. New York.
- Kaluzny, S.P., S.C. Vega, T.P. Cardoso, and A.A. Shelly. 1997. S+ Spatial Stats: A User's Manual for Windows and UNIX. Springer. New York.
- Kronert R., U. Steinhardt, and M. Volks (eds). 2001. Landscape Balance and Landscape Assessment. Springer-Verlag. Berlin.
- Leduc, A., Y.T. Prairie, and Y. Bergeron. 1994. Fractal dimension estimates of a fragmented landscape: sources of variability. *Landscape Ecology*. **9**(4): 279-286.
- Levin, S.A. 1992. The Problem of pattern and Scale in Ecology: The Robert H. MacArthur Award Lecture. *Ecology*. **73**(6): 1943-1967.
- Li, H. and J.F. Reynolds. 1993. A new contagion index to quantify spatial patterns of landscapes. *Landscape Ecology*. **8**: 155-162.
- Mandelbrot, B.B. 1982. The Fractal Geometry of Nature. W. H. Freeman and Co., New York.
- Matousek J. and J. Nesetril. 1988. Invitation to Discrete Mathematics. Oxford University Press, New York.
- McGarigal, K. and B.J. Marks. 1995. FRAGSTATS: spatial pattern analysis program for quantifying landscape structure. Gen. Tech. Report PNW-GTR-351, USDA Forest Service, Pacific Northwest Research Station, Portland, OR.
- McGarigal, K.S., S.A. Cushman, M.C. Neel. And E. Ene. 2002. FRAGSTATS: Spatial Pattern Analysis Program for Categorical Maps. Computer software program produced by the authors at the University of Massachusetts, Amherst.
URL:<http://www.umass.edu/landeco/research/fragstats/fragstats.html>.
- Messina, J.P., K.A. Crews-Meyer, S.J. Walsh. n.d. Scale Dependent Pattern Metrics and Panel Data Analysis as Applied in a Multiphase Hybrid Land Cover Classification Scheme. URL: <http://www.unc.edu/~messina/asprs2000.html>.

Miriam-Webster online dictionary. n.d. URL: <http://www.m-w.com/cgi-bin/dictionary>

O'Neill R.V., C.T. Hunsaker, S.P. Timmins, B.L. Jackson, K.B. Jones, K.H. Riitters and J.D. Wickham. 1996. Scale problems in reporting landscape pattern at regional the regional scale. *Landscape Ecology*. **11**(3): 169-180.

O'Neill, R.V., J.R. Krummel, R.H. Gardner, G. Sigihara, B. Jackson, D.L. DeAngelis, B.T. Milne, M.G. Turner, B. Zygmunt, S.W. Christensen, V.H. Dale, and R.L. Graham. 1988. Indices of landscape pattern. *Landscape Ecology*. **1**: 153-162.

Opdam, P, R. Foppen, and C. Vos. 2002. Bridging the gap between ecology and spatial planning in landscape ecology. *Landscape Ecology*. **16**: 767-779.

Poole, M.A. and P.N. O'Farrell. 1971. The assumptions of the linear regression model. *Transactions of the IBG*, v 52, p 145-158.

Riitters, K., J. Wickham, R. O'Neill, B. Jones, E. Smith. 2000. Global-Scale Patterns of Forest Fragmentation. *Conservation Ecology* **4** (2): 3.
URL:<http://www.consecol.org/vol4/iss2/art3>.

Riitters, K.H., R.V. O'Neill, C.T. Hunsaker, J.D. Wickham, D.H. Yankee, S.P. Timmins, K.B. Jones and B.L. Jackson. 1995. A factor analysis of landscape pattern and structure metrics. *Landscape Ecology*. **10**(1) 23-39.

Riitters, K.H., R. V. O'Neill, J.D. Wickham and K.B. Jones. 1996. A note on contagion indices for landscape analysis. *Landscape Ecology*. **11** (4) 197-202.

Southworth, J., H. Nagendra, and C. Tucker. 2002. Fragmentation of a Landscape: incorporating landscape metrics into satellite analyses of land-cover change. *Landscape Research*. **27**(3), 253-269.

Tate, N.J. and P.M. Atkinson, eds. 2001. Modelling Scale in Geographic Information Science. John Wiley and Sons. Chichester, England.

Tiefelsdorf, M. 2000. Modelling Spatial Processes: The Identification and Analysis of Spatial Relationships in Regression Residuals by Means of Moran's I. Springer-Verlag. Berlin.

Theobald, D.M. Tools Available for Measuring Habitat Fragmentation. URL <http://ndis.nrel.colostate.edu/davet/pubs%5cfragtools.htm>.

Tobler, Waldo R. (1979), Smooth pycnophylactic interpolation for geographical regions, *Journal of the American Statistical Association*, **74**(367):519-530.

Turner, M.G. 1989. Landscape ecology: the effect of pattern on process. *Ann. Rev. Ecol. Syst.* **20**:171-197.

- Turner, M.G. 1990. Spatial and temporal analysis of landscape patterns. *Landscape Ecology*. 4(1) 21-30.
- Turner, M.G., R.H. Gardner, and R.V. O'Neill. 2001. *Landscape Ecology in Theory and Practice: Pattern and Process*. Springer-Verlag. New York.
- Turner, M.G., R.V. O'Neill, R.H. Gardner and B.T. Milne. 1989. Effects of changing spatial scale on the analysis of landscape pattern. *Landscape Ecology*. 3 (3-4) 153-162.
- Vergara, D.G.K. 1997. A Landscape Fragmentation Index for Biodiversity Studies Using GIS. *In* The Conditions of Biodiversity in Asia: The Policy Linkages Between Environmental Conservation and Sustainable Development. M.R. Dove and P.E. Sajise, eds. East-West Center. Hawaii.
- Walker, D., R. Baydack and D. Barber. (n.d.) Biodiversity Values, Sustainable Forest Management. URL.http://www.umanitoba.ca/institutes/natural_resources/biodiversity/biodiversity.html
- Walker, R. (2003). Mapping Process to Pattern in the Landscape Change of the Amazonian Frontier. *Annals of the Association of American Geographers*. 93(2): 376-398.
- Wiangwang, N. 2002. Water clarity/Trophic condition monitoring using Satellite Remote Sensing Data. unpublished M.S. thesis. Michigan State University.
- Wiens, J.A. and B.T. Milne. 1989. Scaling of 'landscapes' in landscape ecology, or, landscape ecology from a beetle's perspective. *Landscape Ecology*. 3(2) 87-96.
- Wu, J. and R Hobbs. 2002. Key issues and research priorities in landscape ecology: An idiosyncratic synthesis. *Landscape Ecology*. 17: 355-365.
- Wu, J., W. Shen, W. Sun, and P. Tueller. 2002. Empirical patterns of the effects of changing scale on landscape metrics. *Landscape Ecology*. 17: 761-782.
- Young, C.H. and P.J. Jarvis. 2001. Measuring urban habitat fragmentation: an example from the Black Country, UK. *Landscape Ecology*. 16: 643 – 658.

REFERENCES

- O'Neill, R.V., A.R. Johnson and A.W. King. 1989. A hierarchical framework for the analysis of scale. *Landscape Ecology*. **3** (3-4): 193-205.
- O'Neill R.V., K.H. Riitters, J.D. Wickham, and K.B. Jones. 1999. Landscape Pattern Metrics and Regional assessment. *Ecosystem Health*. **5** (4): 225-233.
- Qi, W. and J. Wu. 1996. Effects of changing spatial resolution on the results of landscape pattern analysis using spatial autocorrelation indices. *Landscape Ecology*. **11** (1) 39-49.
- Rosen, R. 1989. Similitude, similarity and scaling. *Landscape Ecology*. **3** (3-4) 207-216.
- Turner, M.G., V.H. Dale, R.H. Gardner. 1989b. Predicting across scales: Theory development and testing. *Landscape Ecology*. **3** (3-4) 245-252.

MICHIGAN STATE UNIVERSITY LIBRARIES



3 1293 02504 7873